IMPROVED SYNTHESIS OF COMPUTER GENERATED DIGITAL AMPLITUDE HOLOGRAMS

A DOCTOR OF PHILOSOPHY THESIS

in

Physics

Middle East Technical University

By

GÜVEN, Mehmet Halûk

April 1991

Approval of the Graduate School of Natural and Applied Sciences.

Prof. Dr. O. Alpay Ankara
Director

I certify that I have read this thesis and that in my opinion it is fully adequate, in scope and in quality, as a dissertation for the degree of Doctor of Philosophy.

Prof. Dr. Şinasi Ellialtıoğlu
Chairman of the Department

We certify that we have read this thesis and that in our opinion it is fully adequate, in scope and in quality, as a dissertation for the degree of Doctor of Philosophy.

Prof. Dr. Ramazan Aydın
Supervisor

Examining Committee in Charge:

Prof. Dr. Önder Tüzünalp(Chairman) .....

Prof. Dr. Ramazan Aydın .....

Prof. Dr. Sadrettin Sinman .....

Assoc. Prof. Dr. Gülay Öke .....

Assist. Prof. Dr. Tayfun Arı .....

IMPROVED SYNTHESIS OF COMPUTER GENERATED DIGITAL AMPLITUDE HOLOGRAMS

GÜVEN, Mehmet Halûk

Faculty of Arts and Sciences

Department of Physics, Ph. D. Thesis

Supervisor: Prof. Dr. Ramazan Aydın

57 pages, April 1991

ABSTRACT

A computer generated amplitude hologram is a diffraction object that yields a predefined Fraunhofer diffraction pattern. The object, subject to the hologram, does not have to exist physically.

Calculation of Fraunhofer diffraction pattern by means of computer requires the two dimensional sampled version of the object. The object matrix, then placed in a data matrix. Fast Fourier Transform (FFT) Algoritm is used to calculate diffraction pattern. The off-axis optical holography concepts are applied to plot hologram distribution on the paper. In the next step the distribution is photoreduced on the high resolution photographic plate to produce the hologram. Reconstruction of the image requires an optical set-up. Direct calculation of Fourier spectrum causes high dynamic range as a result most of the information of the reconstructed image is lost. To smooth the dynamic range, diffuse illumination technique of optical holography is simulated by multiplying the elements of the data matrix by random phase factors. The experimental results show that quality of the hologram is deteriorated by random noise, quantization errors and higher diffraction order images. The higher order

images are eliminated by applying the diagonal method, and an Iterative Fourier Transform Algorithm (IFTA) is suggested to produce high quality digital amplitude holograms.

The hologram distributions are also recorded on aluminum applying a photolithographic technique which is explained in detail and experimental results are presented.

Key words : Computer Generated Hologram, Diffuse Illumination, Fast Fourier Transform, Photolithography, Iterative Fourier Transform Algorithm.

Science Code : 404.01.01, 609.02.10

BİLGİSAYARLA GELİŞTİRİLMİŞ SAYISAL GENLİK HOLOGRAMLARININ ÜRETİLMESİ

GÜVEN, Mehmet Halûk

Fen - Edebiyat Fakültesi

Fizik Bölümü, Doktora Tezi

Tez Yöneticisi: Prof. Dr. Ramazan Aydın

57 sayfa, Nisan 1991

ÖZET

Bilgisayarla üretilen sayısal genlik hologramları, daha önce tanımlanmış Fraunhofer kırınım desenini oluşturan optik elemanlardır. Hologramı yapılan nesnenin fiziksel olarak var olması gerekmez.

Fraunhofer kırınım desenini bilgisayarla hesaplayabilmek için nesnenin iki boyutta örneklenmesi gerekir. Nesne matrisi daha sonra veri matrisine yerleştirilir. Kırınım desenini hesaplayabilmek için hızlı Fourier dönüşüm algoritmaları kullanılır. Genlik hologramı üretebilmek için, çizgi dışı hologram savlarından faydalanılarak dağılımı kağıt üzerine çizilir daha sonra bu dağılım yüksek çözümleme gücüne sahip fotoğraf plakalarına kaydedilir.Görüntünün yeniden elde edilebilmesi için özel bir optik düzenek kullanılır. Fourier görünümünün doğrudan hesaplanması, Fourier görünümünde geniş dinamik aralıklara neden olur ve bunun sonucunda elde edilen görüntüdeki çoğu bilgi kaybolur.Bu aralığı azaltmak için optik holografide kullanılan yaygın aydınlatma tekniği, bilgisayarda veri matrisinin elemanlarını rastgele oluşturulmuş faz çarpanları ile çarpılarak canlandırıldı. Deneysel sonuçlar bu şekilde

üretilen hologramlarda rastgele fazın meydana getirdiği gürültü, doğrudan nicemlemeden ileri gelen hatalar ve yüksek mertebe görüntülerin kaliteyi bozduğunu göstermiştir. Yüksek mertebe kırınım görüntüleri çaprazlama tekniği kullanılarak giderilmiş ve bir ardışık yaklaştırım Fourier dönüşüm algoritması yüksek kaliteli hologramlar üretebilmek için önerilmiştir.

Hologram dağılımı fotolitografik teknikler kullanılarak aluminyum üzerine de kaydedilmiştir. Bu tekniğin detayları ve deneysel sonuçlarına da çalışmada yer verilmiştir.

Anahtar kelimeler : Bilgisayarla Üretilmiş Hologram, Yaygın Aydınlatma, Hızlı Fourier Dönüşümü, Fotolitografi, Ardışık Yaklaştırım Fourier Dönüşümü Algoritması.

Bilim Sayısal Kodu : 404.01.01, 609.02.10

ACKNOWLEDGEMENTS

I would like to thank Prof. Dr. Ramazan Aydın and Assist. Prof. Dr. Tayfun Arı for their encouragement, discussions and constant supervision throughout the course of this work.

I am grateful to Prof. Dr. Olof Bryngdahl of Essen University, who is one of the leading scientists in the field CGHs, kindly sent me his collected papers and introduced the different aspects of the field to me.

I am indebted to all of my friends, especially to F. N. Ecevit, S. K. Yerli, İ. Atılgan, and to M. Nakiboğlu for their helps in different stages of this work.

I also thank İ. Aydemir for drawing the figures and H. Yılmaz and Y. Eraydın for photographic and photocopying processes.

Finally, I would like to thank my family, especially my elder sister E. Güven for their patience and interest throughout this work.

TABLE OF CONTENTS

LIST OF FIGURES

Chapter 1

Introduction

Computer generated holograms, synthetic holograms and computer holograms are the terms used to refer to a class of holograms which are produced as graphical output from a digital computer.

Computer generated holograms (CGH) were first described by Brown and Lohmann in 1966 [1]. They explained their task as to find a diffraction object that yield a predefined Fraunhofer diffraction pattern. They produced a Fourier hologram which acts as an optical matched filter when it is inserted into the Fraunhofer plane of a coherent image forming system. Imaging was also demonstrated.

Brown and Lohmann pointed out two important general aspects of computer generated hologram. One aspect is that the objects do not have to exist physically, therefore, idealized wavefronts can be produced. This underlies application of CGH to optical testing and the generation of optical elements. The second aspect is that the image is prescribed and the diffracting object, the hologram is sought as opposite to the usual diffraction problem in which the diffracting object is given and the diffracted field is sought. Thus hologram is connected to inverse scattering.

In CGH some of the production processes are replaced by synthetic ones. Amplitude and phase information of the object is stored into the computer and construction of CGH can be performed in a synthetic way. A comparison between optical and digital holography is illustrated in Fig.1.1.

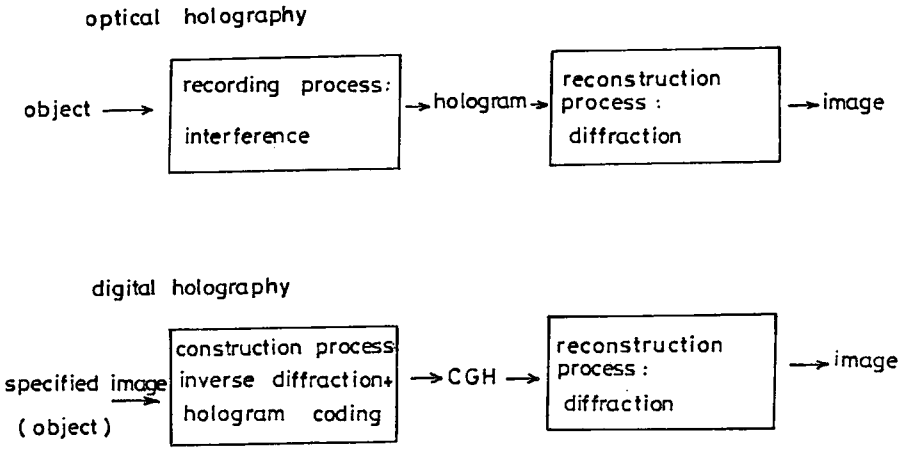

Figure 1.1: Block diagrams indicating the difference between optical and digital holography [2].

Studies on computer generated holography can be roughly divided into three main categories:

i) coding techniques,

ii) applications, and

iii) techniques for improving the quality of computer generated holograms.

The coding of complex wavefronts to make computer generated holograms was first demonstrated by Brown and Lohmann [1] with their detour phase holograms. An interesting aspect of their technique is that the computer generated hologram is made without explicit use of a reference wave or a bias. Also their holograms have only two levels of amplitude transmittance (0 or 1). this makes the holograms easy to produce, and they can be copied many times without degradation.

A different coding method was suggested by Burch in 1967 [3]. As will be explained in detail in Chapter 3, Burch's method is the most convenient technique to produce digital amplitude holograms.

The suggestion of introducing diffuse illumination in optical holography corresponds to superposing a random or quasi random phase [4] onto the specified object in digital holography. Thus the phase in the hologram has a much greater importance than the amplitude. Based on this fact, Lesem, Hirsch and Jordan [5] introduced the idea that a phase mask can be calculated to function as a hologram without a carrier. They called this recording a kinoform, which is a typical digital holography phenomenon in which the phase is not coded indirectly but coded directly and hologram is produced without the introduction of a carrier. The reconstruction from a kinoform does not contain a twin object.Its inherent high efficiency and other characteristics of the fundamental concept were a stimulus to develop this type of digital hologram further.

Lee [6] suggested a hologram encoding scheme, where four real positive functions representing the complex function were sampled with spatial delays. This hologram encoding can be used with implicit carrier and bias.

Application of computer generated holograms can be divided into six areas [7]:

a) production of optical elements,

b) 3-D image display,

c) interferometry,

d) optical memories,

e) optical data processing, and

f) laser beam scanning.

Techniques for improving quality of CGH involve problems such as that of finding the best random phase code or algorithm for reducing the dynamic range in the Fourier transform of an image.

In Chapter 2, the Fourier methods in diffraction theory and Fraunhofer diffraction are reviewed.

In Chapter 3, the fundamental concepts of CGH are introduced. Burch's coding

technique is explained as a simulation of optical off axis holography. To produce CGH the object's Fraunhofer diffraction pattern is calculated by Discrete Fourier Transform (DFT). In these calculations a very powerful algorithm is used, i.e., Fast Fourier Transform (FFT). In this chapter we also explained the successive doubling method of FFT algorithm in one dimension and showed how it can be used in two dimension.

In our study the role of random phase in the production of CGH's are discussed and experimental results are presented in Chapter 4.

One of the methods suggested for the production of high quality CGH's is the Iterative Fourier Transform Algorithm (IFTA) [8]. An iterative algorithm developed in the present study and the experimental results obtained are given in Chapter 5.

In Chapter 6 procedure for recording CGH distribution on Al are given and the results are presented.

Specific reviews on digital holography have been reported by Huang [9], Lee [7], Yaroslavoskii and Merzlyakov [10], Dallas [11], Schreier [12], Tricoles [13], and Bryndahl and Wyrowski [2].

Chapter 2

Fourier Methods in Diffraction Theory

Considering the diffraction of monochromatic light by a finite aperture Σ in an infinite opaque screen [14], [15] involves the problem to find far field flux density

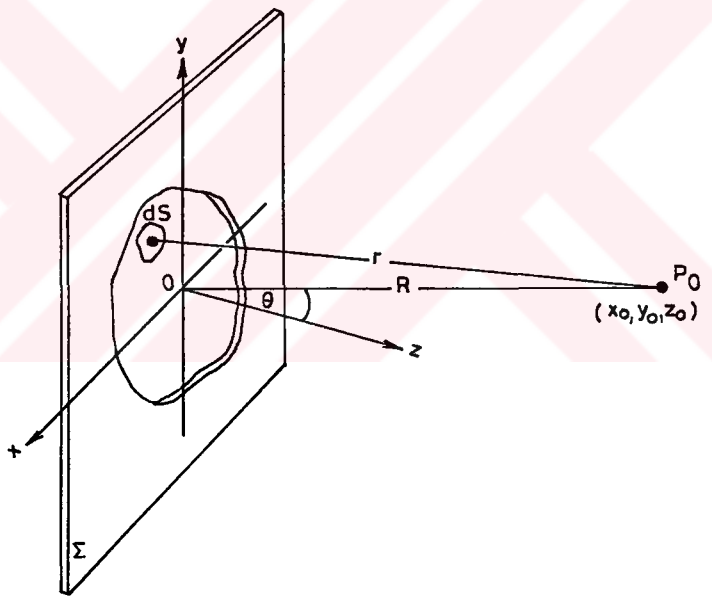

Figure 2.1: Fraunhofer diffraction from an aperture.

distribution at some arbitrary distant point P_0. Assume a differential area dS within the aperture, dS is much smaller than λ, the wavelength of the incoming radiation, in extent and emits a spherical wave. Source strength per unit area over the aperture

is not necessarily constant. Indeed, in general, the field emanating from each area element dS could differ in both amplitude and phase. For example if the aperture were filled with a transparent material, there can be nonuniform absorption as well as a position dependent optical path length through the aperture that will affect the diffracted field distribution. Therefore the field over the aperture is given by a complex aperture function,

$$f(x,y) = \mid f(x,y) \mid e^{i\phi(x,y)} \tag{2.1}$$

The amplitude of the field over the aperture is described by $\mid f(x,y) \mid$ while the phase variation is represented by $e^{i\phi(x,y)}$. Accordingly $f(x,y)dxdy$ is proportional to the diffracted field emanating from the differential source element $dxdy$. Then the optical disturbance at P_0 due to dS, ignoring the time dependence part, is expressed as :

$$dF = \frac{f(x,y)}{r} e^{ikr} dS \tag{2.2}$$

The distance from dS to P_0 is

$$r = [(x_0 - x)^2 + (y_0 - y)^2 + z_0^2]^{1/2} \tag{2.3}$$

and far field (Fraunhofer) condition occurs when r approaches to infinity. Since aperture is small, r may be replaced by R in the amplitude term but in the phase term $k = 2\pi/\lambda$ is a large number and r should be treated carefully. Using

$$R = [x_0^2 + y_0^2 + z_0^2]^{1/2} \tag{2.4}$$

we expand Eq[2.3] as

$$r = R[1 + \frac{x^2 + y^2}{R^2} - \frac{2(xx_0 + yy_0)}{R^2}]^{1/2} \tag{2.5}$$

Fraunhofer condition requires R is very large in comparison to the dimensions of the aperture and the second term in the bracket is negligible. Now

$$r = R[1 - \frac{2(xx_0 + yy_0)}{R^2}]^{1/2} \tag{2.6}$$

and in the binomial expansion dropping all but the first two terms we have

$$r = R[1 - \frac{(xx_0 + yy_0)}{R^2}] \tag{2.7}$$

Thus the total disturbance arriving at P_0 is

$$F = \frac{e^{ikR}}{R} \int\int_{aperture} f(x,y) \exp[\frac{-ik(xx_0 + yy_0)}{R}] dS \tag{2.8}$$

The $1/R$ corresponds to the drop off of the field amplitudes with distance from the aperture and e^{ikR} is an unimportant phase factor. Thus if we limit ourselves to a small region of output space over which R is constant everything in front of the integral can be regarded as a constant. So Eq[2.8] can be rewritten as

$$F = \int_{-\infty}^{\infty}\int_{-\infty}^{\infty} f(x,y) e^{\frac{-ik(xx_0+yy_0)}{R}} dxdy \tag{2.9}$$

It might be helpful to envision $dF(x,y)$ at a given point P_0 as if it were a plane wave propagating in the direction of $\vec{k}$ as shown in Fig(2.2).

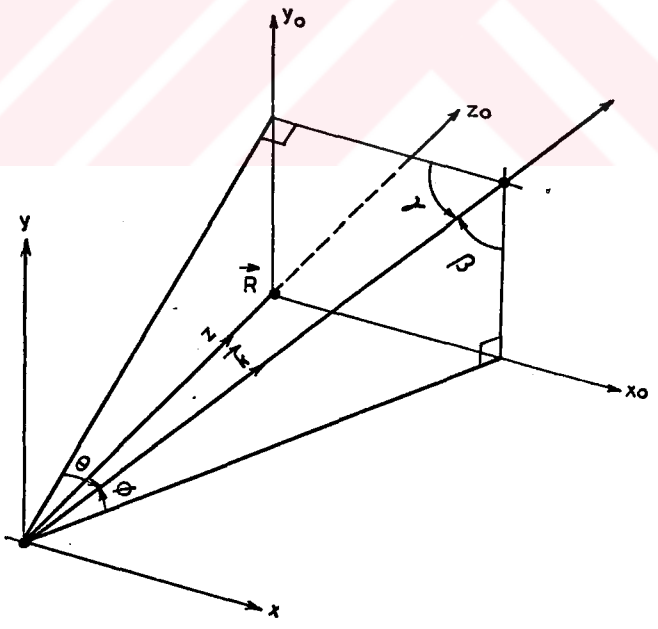

Figure 2.2: Geometry of the discussion.

Let's define the spatial frequency u and v as

$$u = \frac{kx_0}{R} = k\sin(\theta) = k\cos(\gamma) \tag{2.10}$$

$$v = \frac{ky_0}{R} = k\sin(\phi) = k\cos(\beta) \tag{2.11}$$

For each point on the image plane, there is a corresponding spatial frequency. The diffracted field can now be written as

$$F(u,v) = \int_{-\infty}^{\infty}\int_{-\infty}^{\infty} f(x,y)e^{-i(ux+vy)}dxdy \tag{2.12}$$

and we have arrived the key point: the field distribution in the Fraunhofer diffraction pattern is the Fourier Transform (FT) of the field distribution across the aperture.

Symbolically this is written as :

$$F(u,v) = FT[f(x,,y)] \tag{2.13}$$

The field distribution in the image plane is the spatial frequency spectrum of the aperture function. The inverse transform is then

$$f(x,y) = \frac{1}{(2\pi)^2}\int_{-\infty}^{\infty}\int_{-\infty}^{\infty} F(u,v)e^{i(ux+vy)}dudv \tag{2.14}$$

or,

$$f(x,y) = FT^{-1}[f(u,v)] \tag{2.15}$$

Chapter 3

Fundamentals of Computer Generated Holography

In digital holography, hologram recording is performed synthetically supported by digital computer means, and the reconstruction step remains just the same as in optical holography. The procedure begins with a specified object (reconstructed image) and an inverse diffraction is performed to determine the complex amplitude that will be recorded later in the hologram. Thus in digital holography the following steps should be considered :

i) Calculation of the complex amplitude in the hologram plane from specifications of the reconstruction. In general the starting point is to specify the desired wavefront or data of 1-D, 2-D, or 3-D in the reconstruction space. The statement of the reconstructed wavefield or object has to be in an optical form and the proper style for computer handling. The optical quantities of amplitude and phase (and/or) polarization, frequency can be in a continuous or sampled form. This specification is succeeded by a transformation (image, Fresnel, Fourier), which can be realized by inverse wave propagation methods. As a result, the amplitude and phase are obtained, usually in sampled form, in the hologram plane.

ii) Generation of the hologram. The amplitude to be stored in the hologram is converted to a CGH configuration of analog or quantized values. Practical and physical constraints will guide the choice of procedure for realization. A coding

scheme is applied to make the CGH structure conform to requirements of material and recording devices. As a result, the complex amplitude to be stored in the CGH can be encoded in a real and positive valued distribution or in a phase only distribution to adopt to recording media.

iii) Optical reconstruction. Proper illumination of the CGH results in a reconstruction of the object (data) as a light distribution. It is customary in this process to regard the CGH as a thin hologram. As a result of the specific properties of the CGH's, the reconstruction will show certain characteristics. Sampling and quantization especially demonstrate typical features. The specification of the object and hologram type leads to possible coding schemes in the actual application.

The strength of digital holography results from the flexibilities of the first two synthetic steps, which posses extra freedoms that can not be exercised by optical process. To circumvent difficulties in the treatment of 3-D light distribution in the first step, models are introduced in digital holography. Frequently holography is incorporated in a larger connection and system aspect prevail. This is evident in the execution of the first two steps by adaptation to specific application needs and physical hardware as well as to existing computer hardware and software.

The initial step in the realization of CGH is to define the desired distribution to be reconstructed, which will be called object. The object needs to be specified in such a way that the relation, which is an inverse wave propagation relation, between it and the distribution in the hologram plane can be calculated by a digital computer. The transformation from object to hologram is determined by the dimensionality of the object and the distance between the object and the hologram. The object may be described as a 1-D, 2-D or 3-D continuous or discrete distribution of complex amplitudes depending on the CGH application. The object may be located in the far, mean, or even within the field of the hologram, and a Fourier, Fresnel, or no transform is necessary to determine the distribution in the hologram plane.

In this work we are concerned with the Fourier type inverse wave propagation and resulting transformation object and hologram.

The aim of Fourier holography is to form a light distribution of a desired reconstructed image (object) in the Fourier plane of the hologram. A distinction is made between objects and intensity objects.

The distribution of an object in the form of a complex amplitude

$$f(\vec{x}) = \mid f(\vec{x}) \mid e^{[i\phi(\vec{x})]} \tag{3.1}$$

for a complex object and in the form of intensity

$$\mid f(\vec{x}) \mid^2 = i(\vec{x}) \tag{3.2}$$

for an intensity object, where $\vec{x} = (x, y)$ and $arg[f(\vec{x})] = \phi(\vec{x})$. For an intensity object any complex amplitude

$$f(\vec{x}) = [i(\vec{x})]^{(1/2)} e^{[i\phi(\vec{x})]} \tag{3.3}$$

with the arbitrary phase $\phi(\vec{x})$ will lead to Eq[3.2] which implies that $\phi(\vec{x})$ can be chosen freely, i.e., $f(\vec{x})$ is not fixed.

In both Eq[3.1] and Eq[3.2], $f(\vec{x})$ determines the object. The aim is to calculate the complex amplitude $F(\vec{u})$ in the hologram plane, which is transformed into the complex amplitude $f(\vec{x})$ in the reconstruction plane. In Fourier holography this transformation is a Fourier transform (FT) of $f(\vec{x})$, i.e.,

$$F(\vec{u}) = FT[f(\vec{x})] = \int_{-\infty}^{\infty} f(\vec{x}) e^{-2\pi i \vec{u} \cdot \vec{x}} d\vec{x} \tag{3.4}$$

where $\vec{u} = (u, v)$ and $\vec{u} \cdot \vec{x} = ux + vy$.

Eq[3.4] describes the relationship between the object $f(\vec{x})$ and its spectrum $F(\vec{u})$, and the conditions of digital Fourier holography are determined by this inter-relationship.

3.1 Boundary Conditions of Spectrum and Object

For performing the Fourier transform the object function $f(\vec{x})$ is represented by an array of its sampled values taken on a discrete set of point in xy-plane. This is convenient both for data processing and for mathematical analysis, to represent $f(\vec{x})$ by an array of its sampled values taken on a discrete set of points in the xy-plane. Intuitively, it is clear that if these samples are taken sufficiently close to each other, the sampled data are an accurate representation of the original function in the sense that can be reconstructed with considerable accuracy by simple interpolation. It is less obvious fact that for a particular class of functions (known as band-limited functions) the reconstruction can be accomplished exactly, providing only that the interval between samples is not greater than a certain limit [16,17].

By band-limited functions we mean functions with Fourier transforms nonzero over only a finite region of the u space.

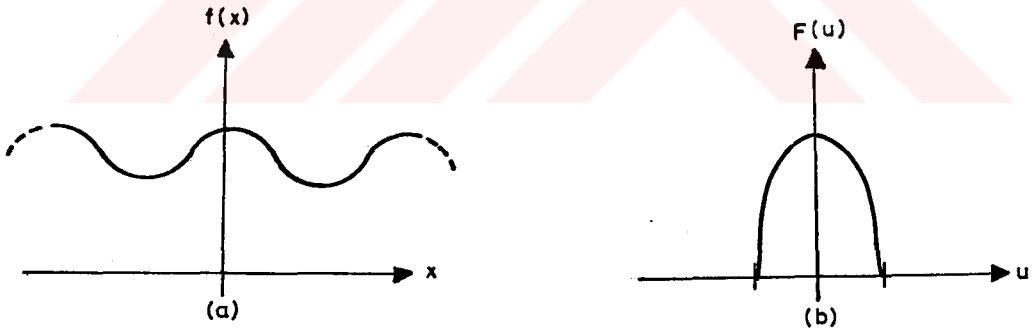

Figure 3.1: Illustration of band limited function.

In the object plane, sampling of $f(\vec{x})$ is not a problem because $\Delta\vec{F} < \infty$ where $\Delta\vec{F}$ is the size of $F(\vec{u})$, $\Delta\vec{F} = (\Delta F_u, \Delta F_v)$. A sampled (discrete) version of $f(\vec{x})$ is introduced as follows :

$$f(\vec{m}) := f(m\delta x, n\delta y) = f(\vec{x})comb(\vec{x}, \delta\vec{x}) \tag{3.5}$$

with integers $\vec{m} = (m, n)$, a sampling distance $\delta\vec{x} = (\delta x, \delta y)$ and,

$$comb(\vec{x}, \vec{a}) \sim \sum_{\alpha,\beta=-\infty}^{\infty} \delta(x - \alpha a)\delta(y - \beta b) \tag{3.6}$$

where $\vec{a} = (a, b)$, and $\delta(\vec{x})$ is the Dirac delta function.

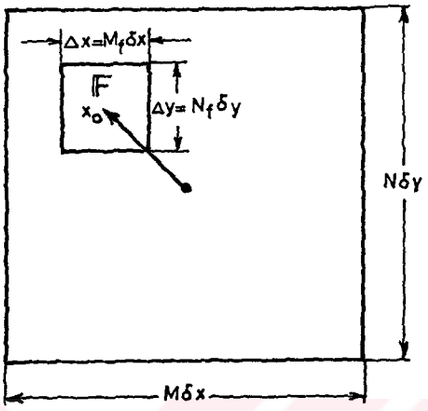

Figure 3.2: Illustration of the notation on the data matrix.

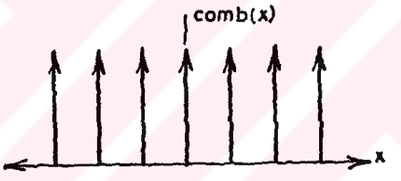

Figure 3.3: One dimensional *comb* function.

As long as $\delta x \leq (\Delta F_u)^{-1}$ and $\delta y \leq (\Delta F_v)^{-1}$ or in vectorial form $\delta\vec{x} \leq (\Delta\vec{F})^{-1}$ the sampling is correct according to the sampling theorem.

A discrete object is given as a 2-D set of data in $M_f N_f$ points. It is interpreted as a discrete version or a complex amplitude $f(\vec{x})$; i.e., as $f(\vec{m}_f)$. Thus the complex amplitude $f(\vec{x})$ is only defined in the sampling points.

A possible choice of $f(\vec{x})$ is

$$f(\vec{x}) = \sum_{\vec{m}_f} f(\vec{m}_f) sinc[\frac{x - m_f \delta x}{\delta x}]\ sinc[\frac{y - n_f \delta y}{\delta y}] \tag{3.7}$$

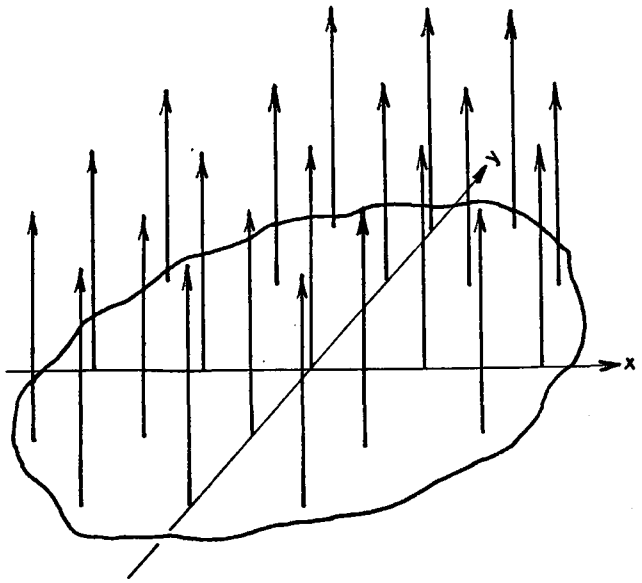

Figure 3.4: The sampled function.

or in abbreviated form

$$f(\vec{x}) = f(\vec{m_f}) * sinc(\vec{x}, \delta\vec{x}) \tag{3.8}$$

with

$$sinc(\vec{x}, \vec{a}) \sim \frac{sin(\pi x/a)}{\pi x/a} \frac{sin(\pi y/b)}{\pi y/b} \tag{3.9}$$

whereby $\vec{a} = (a, b)$. This means that $f(\vec{x})$ is introduced as the sinc interpolation of the values $f(\vec{m_f})$.

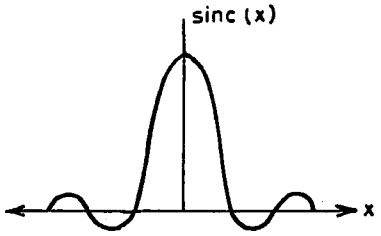

Figure 3.5: Sinc function.

The choice of Eq[3.8] satisfies both boundary conditions, i.e.,

i) $\Delta x = (M_f \delta x, N_f \delta y) < \infty$ and

ii) $\Delta\vec{F} = (\delta\vec{x})^{-1} < \infty$.

The actual procedure is to start from $f(\vec{m}_f)$ to calculate $F(\vec{k})$ and then perform the coding, the CGH production, and the optical reconstruction.

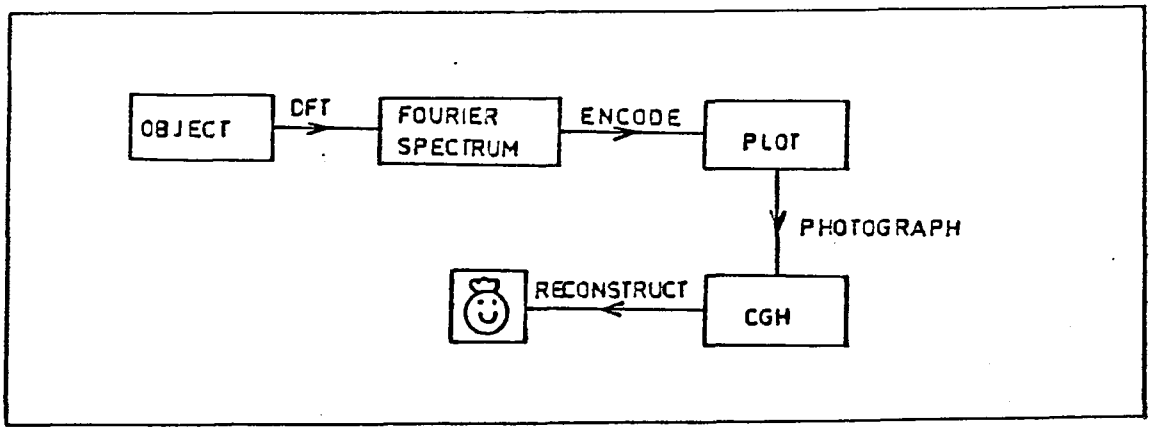

Figure 3.6: Block diagram showing the different steps in the realization of CGH.

In considering the effect of aliasing, we disregard the coding and the production steps and assume that reconstruction follows directly after $F(\vec{k})$. Then,

$$FT^{-1}[F(\vec{k})] = FT^{-1}[F(\vec{u})comb(\vec{u}, \delta\vec{u})] = f(\vec{x}) * comb(\vec{x}, \delta\vec{u}^{-1}) \qquad (3.10)$$

i.e., repetition occurs. Thus $\Delta\vec{f} = \infty$ causes superposition (aliasing).

However, in the case $\delta\vec{u}^{-1} = (\alpha\delta x, \beta\delta y)$, where α, β are integers, the discrete distribution $f(\vec{m}_f)$ is contained undisturbed in $f(\vec{x})$ because the zeros of the sinc function of Eq[3.9] are located in the sampling points.

In practice, $\alpha = M_f$ and $\beta = N_f$ are chosen, i.e., $\delta\vec{u}^{-1} = (M_f\delta x, N_f\delta y)$, or multiples thereof. The values in the sampling points are then correct and aliasing is not disturbing.

After discussing the aliasing problem for discrete object we turn back to the problem of sampling in the hologram plane. In analogy to Eq[3.5] it is necessary to

sample

$$F(\vec{k}) := F(k\delta u, l\delta v) = F(\vec{u})comb(\vec{u}, \delta\vec{u}) \tag{3.11}$$

where $\vec{k} = (k, l)$ and $\delta\vec{u} = (\delta u, \delta v)$.

A computer is used combine $f(\vec{m})$ and $F(\vec{k})$, this means that the number of points needs to be limited.

According to the constraints $\Delta\vec{F} < \infty$ and $\Delta\vec{x} < \infty$ the sampled version of $F(\vec{u})$ and $f(\vec{x})$ are connected by the discrete Fourier transform,

$$F(\vec{k}) = \sum_{\vec{m}}^{\vec{M}} f(\vec{m}) \exp[-2\pi i(\frac{\vec{k} \cdot \vec{m}}{\vec{M}})] \tag{3.12}$$

The connection between the sampling distance $\delta\vec{u}$ and $\delta\vec{x}$ is

$$\delta\vec{u} = (\Delta\vec{x}^{-1}) = [(M\delta x)^{-1}, (N\delta y)^{-1}] \tag{3.13}$$

In digital holography, there is no reason to choose $\delta\vec{x} < \Delta\vec{F}^{-1}$ to oversample in the $\vec{x}$ plane. Hence, the object is sampled at its Nyquist rate $\delta\vec{x} = \Delta\vec{F}^{-1}$. To indicate $\vec{m}_f$ and $\vec{M}_f$ are introduced ;

$$f(\vec{m}_f) = f(\vec{x})comb(\vec{x}, \Delta\vec{F}^{-1}) \tag{3.14}$$

with $\vec{m}_f = -1/2\vec{M}_f, ..., 1/2\vec{M}_f - \vec{1}$ where $\vec{M}_f = (\Delta x/\delta x, \Delta y/\delta y) = (\Delta x\Delta F_u, \Delta y\Delta F_v)$.

The discrete Fourier transform (DFT) of $f(\vec{m}_f)$ results in the corresponding discrete spectrum $F(\vec{k}_f)$ with $\vec{k}_f = -1/2\vec{M}_f, ..., 1/2\vec{M}_f - \vec{1}$.

According to the Eq[3.13] $\delta\vec{u} = \Delta\vec{x}^{-1}$ is valid independent of $\delta\vec{x}$. Then in regard to $\Delta\vec{x} < \infty$ the spectrum $F(\vec{u})$ is sampled with the largest possible distance $\delta\vec{u}$.

However, for various reasons (aliasing in reconstruction coding etc.) it is helpful to use $\delta\vec{u} < \Delta\vec{x}^{-1}$. This is realized by embedding $f(\vec{m}_f)$ in a MN data field matrix of zero. The DFT will result in

$$F(\vec{k}) = F(\vec{u})comb(\vec{u}, \delta\vec{u}) \tag{3.15}$$

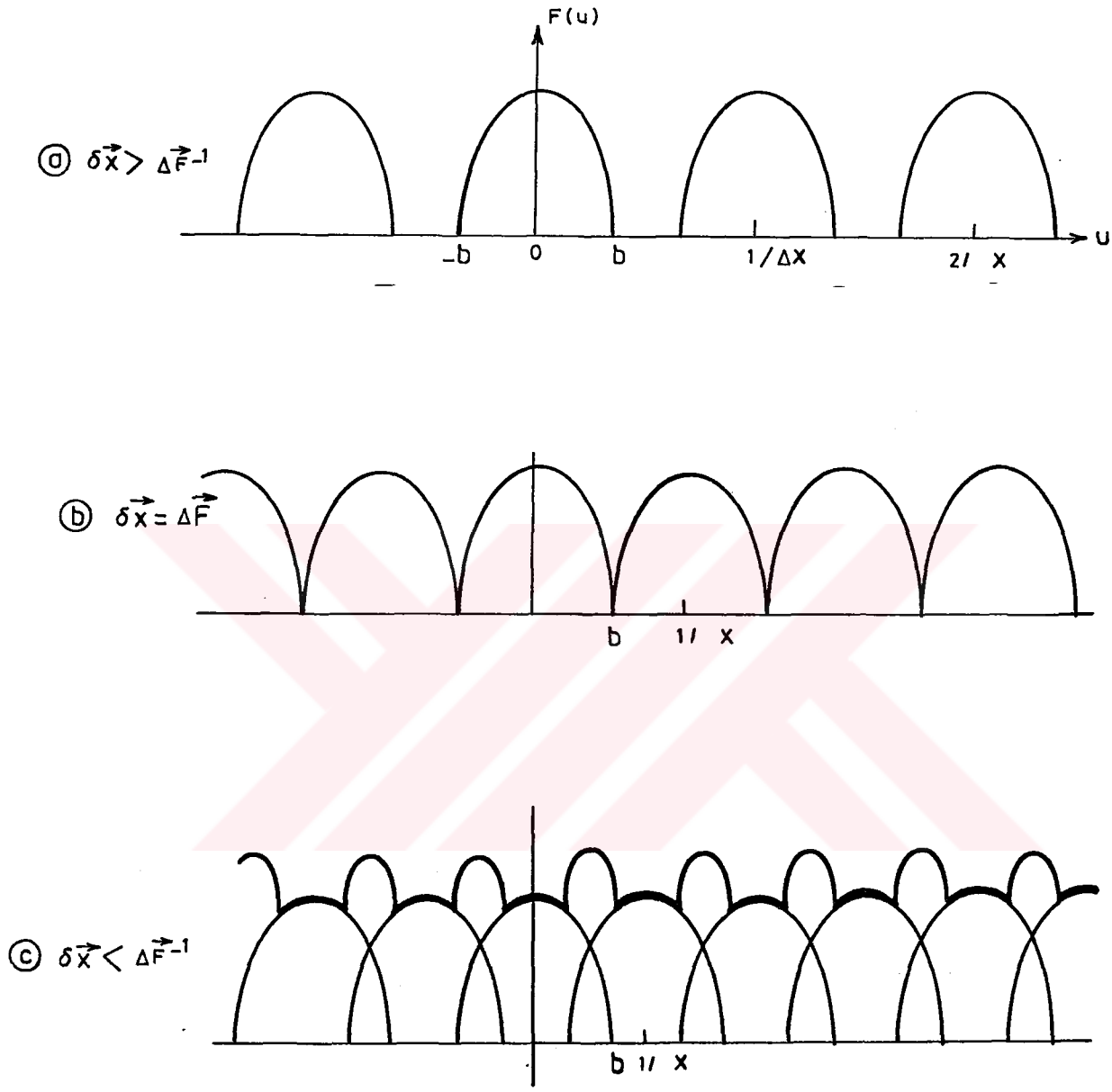

Figure 3.7: Representation of a) over sampling, b) sampling at Nyquist rate and c) aliasing cases.

with $\vec{k} = -1/2\vec{M}, .., 1/2\vec{M} - \vec{1}$, and $\delta(\vec{u}) = [(M_f/M\Delta x^{-1}), (N_f/N)\Delta y^{-1})]$; this means an oversampling in regard to $\Delta\vec{x}$ with M/M_f in the u direction and N/N_f in the v direction.

In short, in case

i) $\Delta\vec{x} < \infty$ and

ii) $\Delta\vec{F} < \infty$ are secured an arbitrarily sampled version of the desired $F(\vec{u})$, i.e.,$F(\vec{k})$ is obtained by a DFT of $f(\vec{m}_f)$ whereby the DFT is implemented by the FFT algorithm.

3.2 Two Dimensional Discrete Fourier Transform

In the two dimensional case the discrete Fourier pair is given by the equations

$$F(k,l) = \frac{1}{MN}\sum_{m=0}^{M-1}\sum_{n=0}^{N-1} f(m,n)\exp[-2\pi i(\frac{km}{M} + \frac{ln}{N})] \tag{3.16}$$

and

$$f(m,n) = \sum_{k=0}^{M-1}\sum_{l=0}^{N-1} F(k,l)\exp[2\pi i(\frac{km}{M} + \frac{ln}{N})] \tag{3.17}$$

The continuous function sampled in a two dimensional grid with divisions of width δx and δy in the x and y axis respectively. The sampling increments in the spatial and frequency domains are related by

$$\delta u = \frac{1}{M\delta x} \tag{3.18}$$

and

$$\delta v = \frac{1}{N\delta y} \tag{3.19}$$

When the images are sampled in a square array we have $M = N$ and

$$F(k,l) = \frac{1}{M}\sum_{m=0}^{M-1}\sum_{n=0}^{M-1} f(m,n)\exp\{-2\pi i[\frac{(km+ln)}{M}]\} \tag{3.20}$$

$$f(m,n) = \frac{1}{M}\sum_{k=0}^{M-1}\sum_{l=0}^{M-1} F(k,l)\exp\{2\pi i[\frac{(km+ln)}{M}]\} \tag{3.21}$$

Note that in this case we have included a $1/M$ term in both expressions. Since $F(k,l)$ and $f(m,n)$ are Fourier transform pair, the grouping of these constant multiplicative terms is arbitrarily.

3.3 The Fast Fourier Transform

In this part Fast Fourier Transform (FFT) algorithm will be explained for one variable and then explained how a two dimensional Fourier transform can be computed by a series applications of the one dimensional transform.

Direct calculation of Fourier transform requires N^2 complex multiplications and additions,

$$F(k) = \frac{1}{M} \sum_{m=0}^{M-1} f(m) \exp[-2\pi i \frac{km}{M}] \tag{3.22}$$

where $F(k)$ and $f(m)$ are complex quantities.

Properly composing the Eq[3.22] the number of multiply and add operations can be made to proportional to $N \log_2 N$. The composition procedure is called the Fast Fourier Transform (FFT) algorithm.

The FFT algorithm used in our calculations is based on the so called " successive doubling method ". It will be convenient to express Eq[3.22] in the form

$$F(k) = \frac{1}{M} \sum_{m=0}^{M-1} f(m) W_M^{km} \tag{3.23}$$

where

$$W_M = e^{-\frac{2\pi i}{M}} \tag{3.24}$$

and M is assumed to be of the form

$$M = 2^n \tag{3.25}$$

where n is a positive integer so we can express N as

$$M = 2N \tag{3.26}$$

where M is also a positive integer. Substitution of Eq[3.26] into Eq[3.23] yields

$$F(k) = \frac{1}{2N}\sum_{m=0}^{2N-1} f(m)W_{2N}^{km} = \frac{1}{2}\{\frac{1}{N}\sum_{m=0}^{N-1} f(2m)W_{2N}^{k(2m)} + \frac{1}{2}\frac{1}{N}\sum_{m=0}^{N-1} f(2m+1)W_{2N}^{k(2m+1)}\} \tag{3.27}$$

From Eq[3.24], $W_{2N}^{2km} = W_N^{km}$ then Eq[3.27] may be expressed in the form

$$F(k) = \frac{1}{2}\{\frac{1}{N}\sum_{m=0}^{N-1} f(2m)W_N^{km} + \frac{1}{N}\sum_{m=0}^{N-1} f(2m+1)W_N^{km}W_{2N}^{k}\} \tag{3.28}$$

if we define

$$F_{even}(k) = \frac{1}{N}\sum_{m=0}^{N-1} f(2m)W_N^{km} \tag{3.29}$$

for $k = 0, 1, 2, ..., N-1$ and

$$F_{odd}(k) = \frac{1}{N}\sum_{m=0}^{N-1} f(2m+1)W_N^{km} \tag{3.30}$$

for $k = 0, 1, 2, ..., N-1$ then Eq[3.28] becomes

$$F(k) = \frac{1}{2}\{F_{even}(k) + F_{odd}(k)W_{2N}^{k}\} \tag{3.31}$$

Also, since $W_N^{k+N} = W_N^k$ and $W_{2N}^{k+N} = -W_{2N}^k$, it follows from Eq[3.29] and Eq[3.31] that

$$F(k+N) = \frac{1}{2}\{F_{even}(k) - F_{odd}(k)W_{2N}^{k}\} \tag{3.32}$$

Equations [3.29] through [3.32] reveals some interesting properties of these expressions. It is noted that an N-point transform can be computed by dividing the original expression into two parts, as indicated in Eqs[3.31] and [3.32]. Computation of the first half of $F(k)$ requires the evaluation of the two $(M/2)$ point transforms given in Eqns[3.29] and [3.30]. The resulting values of $F_{even}(k)$ and $F_{odd}(k)$ are then substituted into Eq[3.31] to obtain $F(k)$ for $k = 0, 1, 2, ...(M/2-1)$. The other half then follows directly from Eq[3.32] without additional transform evaluations.

Implementation of Eqs[3.29] through [3.32] constitutes the successive doubling FFT algorithm. This name arises from the fact that a two point transform is computed from two one point transforms, a four point transform from two point transforms, and so on, for any M that is equal to an integer power of 2.

The Fortran subroutines for an implementation of the successive doubling FFT algorithm is given below. The subroutine was used in our calculations [18].

```
      SUBROUTINE FFT(F,LN)
      COMPLEX F(1024),U,W,T,CMPLX
      PI=3.141593
      N=2**LN
      NV2=N/2
      NM1=N-1
      J=1
      DO 3 I=1,NM1
      IF(I.GE.J)GOTO 1
      T=F(J)
      F(J)=F(I)
      F(I)=T
1     K=NV2
2     IF(K.GE.J) GOTO 3
      J=J-K
      K=K/2
      GOTO 2
3     J=J+K
      DO 5 L=1,LN
      L=2**L
      LE1=LE/2
      U=(1.0,0.0)
      W=CMPLX(COS(PI/LE1),-SIN(PI/LE1))
      DO 5 J=1,LE1
      DO 4 I=J,N,LE
```

```
      IP=I+LE1
      T=F(IP)*U
      F(IP)=F(I)-T
4     F(I)=F(I)+T
5     U=U*W
6     F(I)=F(I)/FLOAT(N)
      RETURN
      END
```

3.4 Two Dimensional FFT

The FT of a discrete function

$$F(k,l) = \frac{1}{M}\sum_{m=0}^{M-1}\sum_{n=0}^{M-1} f(m,n)\exp[-2\pi i\frac{(km+ln)}{M}] \tag{3.33}$$

can be expressed in the separable form

$$F(k,l) = \frac{1}{M}\sum_{m=0}^{M-1} F(m,l)\exp[-2\pi i\frac{mk}{M}] \tag{3.34}$$

where

$$F(m,l) = M[\frac{1}{M}\sum_{n=0}^{M-1} f(m,n)\exp[-2\pi i\frac{ln}{M}] \tag{3.35}$$

For each value of m, the expression inside the brackets is a one dimensional transform. Therefore the two dimensional function $F(m,l)$ is obtained by taking a transform along each row of $f(m,n)$ and multiplying the result by M. The desired result, $F(k,l)$ is then obtained by taking a transform along each column of $F(m,l)$ as in Eq[3.34]. The procedure is shown in Fig[3.7].

It should be noted that the same results would be obtained by first taking transforms along the columns of $f(m,n)$ and then along the rows of the result.

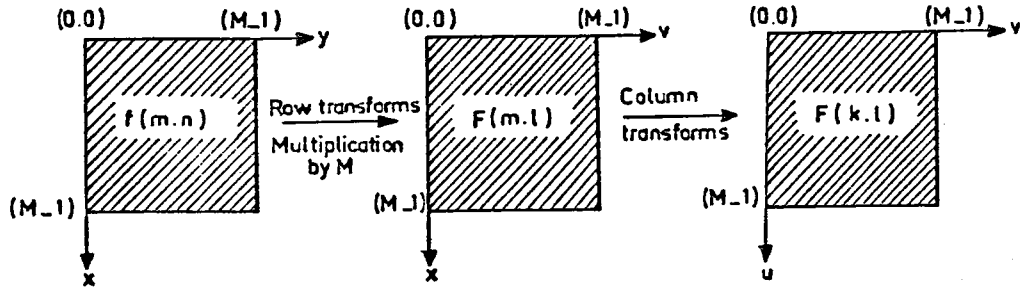

Figure 3.8: Computation of two dimensional FT as a series of one dimensional FT.

3.5 The Inverse FFT

$$F(k,l) = \frac{1}{M}\sum_{m=0}^{M-1}\sum_{n=0}^{M-1} f(m,n)\exp[-2\pi i\frac{(km+ln)}{M}] \tag{3.36}$$

$$f(m,n)\frac{1}{M}\sum_{k=0}^{M-1}\sum_{l=0}^{M-1} F(k,l)\exp[2\pi i\frac{(km+ln)}{N}] \tag{3.37}$$

Taking the complex conjugate of Eq[3.37] we obtain

$$f^*(m,n) = \frac{1}{M}\sum_{k=0}^{M-1}\sum_{l=0}^{M-1} F^*(k,l)\exp[2\pi i\frac{(km+ln)}{M}] \tag{3.38}$$

By comparing this result with Eq[3.36] we see that the right hand side of Eq[3.38] is in the form of the forward Fourier transform. It therefore follows that if we input $F^*(k,l)$ into an algorithm designed to compute the forward transform, the result will be $f^*(m,n)$. By taking the complex conjugate of this result we obtain $f(m,n)$.

3.6 Encoding The Fourier Spectrum

Among a number of techniques available for encoding the object Fourier spectrum, most notably Lohmann's and Lee's methods can be mentioned. But to produce digital amplitude holograms the most convenient technique is that of the Burch's method [3].

In Fourier holography a Fourier transform (FT) relationship exists between the hologram distribution and its diffraction pattern. To obtain the signal $f(\vec{x})$ as the

Fraunhofer pattern, it is necessary to realize the distribution

$$F(\vec{u}) = FT[f(\vec{x})] \tag{3.39}$$

as a transparency. In general the spectrum $F(\vec{u})$ is a complex valued distribution. Thus $F(\vec{u})$ can not be realized directly as an amplitude hologram. It is necessary to encode $F(\vec{u})$ in a real and positive valued distribution. Using a reference wave as in the case of optical hologram is a way to encode the Fourier spectrum which was offered by Burch in 1967. Having calculated the light wave $f(\vec{x})$ due to the object, we add a reference wave $b(\vec{x})$ to it, and square the absolute value of the sum to get

$$h(\vec{x}) = \mid f(\vec{x}) + b(\vec{x}) \mid^2 \tag{3.40}$$

where $f(\vec{x}) = \mid f(\vec{x}) \mid e^{i\phi}$.

The reference wave can be a plane wave, in this case

$$h(\vec{x}) = \mid f(\vec{x}) + be^{iu\vec{x}} \mid^2 \tag{3.41}$$

$$h(\vec{x}) = f^2 + b^2 + 2f(\vec{x})b\cos(u\vec{x} - \phi) \tag{3.42}$$

where b and u are real constants. We then produce a film transparency with an amplitude proportional to $h(\vec{x})$, which is real and positive.

To reconstruct optically, we have a plane wave $Be^{(iu\vec{x})}$ incident upon the hologram, producing a light wave that contains four components. Two of the components are, respectively , proportional to $f(\vec{x})$ the original wave and $f^*(\vec{x})e^{2iu\vec{x}}$, where $*$ denotes complex conjugation. The other two components constitute noise; i.e., they are undesired. We note that two desired components are due to the last term at the right handside of Eq[3.42]. As far as we are concerned, the first two terms at the right-hand side of Eq[3.42] are there for the sole purpose of biasing, i.e., making $h(\vec{x})$ positive for all (x, y) so that we can record it on film as a density variation. In making holograms optically, the use of $(f^2(\vec{x}) + B^2)$ as the bias is convenient, since Eq[3.41]

is easy to perform by photooptical means. However when we make holograms on the computer, we are much more flexible. We can use other forms of biases.

Burch suggested the use of a constant bias, yielding the hologram

$$h(x,y) = K + 2Bf(\vec{x})\cos[u\vec{x} - \phi(\vec{x})] \tag{3.43}$$

where K is a constant which is just large enough to make $h(\vec{x})$ positive for all (x,y).

The advantage of Burch's hologram is that the noise component in the reconstruction is just a plane wave.

Chapter 4

Computer Generated Digital Amplitude Holograms

4.1 Fundamental Principles

Digital Fourier holograms are in the shape of transmission masks which are used to generate Fraunhofer diffraction pattern. They are employed as filters in optical image processing systems. Moreover, they may be applied as optical elements, e.g., in optical memories and as beam profile converters [7].

The first step in the production process of a digital hologram is the determination of the hologram transmission, which will form the desired diffraction pattern. This pattern contains signal. When the signal is expressed by the complex amplitude $f(\vec{x}) =\mid f(\vec{x}) \mid \exp[i\phi(\vec{x})]$, the spectrum $F(\vec{u}) =\mid F(\vec{u}) \mid \exp[i\Phi(\vec{u})] = FT[f(\vec{x})]$ constitutes a suitable transmission to form a Fourier hologram. The Fourier transform of $f(\vec{x})$ can be calculated as a discrete Fourier transform with the values of the amplitude and phase of $F(\vec{u})$ stored as a data set in the computer memory. From this data set one may proceed to the next hologram production step. The spectrum $F(\vec{u})$ is a complex valued function and possesses the following properties:

i) its extent is finite,

ii) it can be transformed into the desired reconstruction $f(\vec{x})$ by inverse transform.

$F(\vec{u})$ is usually given in the discrete form $F(\vec{k}) = F(\vec{u})comb(\vec{u}, \delta\vec{u})$ and from this expression CGH pattern is calculated. Thus $F(\vec{u})$ contains a transformed version of the information of the object $f(\vec{x})$ which is regenerated by illuminating the hologram. In the case of the thin holograms, hologram distribution is directly related to the complex refractive index of the hologram material. Hologram is illuminated by a monochromatic plane wave as a result the complex amplitude $F(\vec{u})$ has to be recorded as a hologram distribution.

It is generally complicated to influence the amplitude as well as the phase of an illumination wave directly. Therefore, the application of techniques and materials which do not rely on complex valued quantities is the standard procedure to produce CGHs. These methods may be grouped according to the parameter of the illuminating wave being influenced as amplitude and phase holograms. The purpose of the coding step is to transfer the complex valued distribution $F(\vec{u})$ into a new distribution $G(\vec{u})$, the values of which are being real and positive.

The transfer from $F(\vec{u})$ to $G(\vec{u})$ will restrict the set of values of $F(\vec{u})$, and one has to make sure that the object distribution $f(\vec{x})$ is included in the distribution

$$T^{-1}[G(\vec{u})] = g(\vec{x}) \tag{4.1}$$

this means the transformed information about the object must be contained in $G(\vec{u})$.

In order to carry out the coding, there should be some kind of freedom. An accurate coding is not possible under the requirement that $F(\vec{u})$ is the unique complex amplitude in the hologram plane which contains the object information. The distribution in the hologram plane should incorporate freedoms; it should in principle be possible to transfer $F(\vec{u})$ into $G(\vec{u})$ without destroying the object information.

4.2 Actual Procedure to Produce Computer Generated Digital Amplitude Holograms

To obtain the signal $f(\vec{x})$ as the Fraunhofer pattern, it is necessary to realize the distribution

$$F(\vec{u}) = FT[f(\vec{x})] \tag{4.2}$$

as a transparency. The calculation method involves the usual procedure of coding the image into a two dimensional matrix and obtaining its Fourier transform. According to the familiar DFT definition.

$$F(\vec{k}) = \frac{1}{M} \sum_{m=0}^{M-1} \sum_{n=0}^{M-1} f(\vec{m}) \exp[-2\pi i(\frac{km + ln}{M})] \tag{4.3}$$

where $F(\vec{k}) = F(k,l)$ represents an element of the Fourier transformed matrix, and $f(\vec{m})$ is an element of the object matrix.

As a signal $f(\vec{x})$, we choose a letter, i.e., " F " it is then sampled in a 32x32 matrix. This sampled signal $f(\vec{m}_f)$ is embedded at the position, $\vec{m}_0 = (-32, 32)$ into a data field of M^2 zeros where $M = 128$. The resulting data set is indicated by $g(\vec{m})$ with $\vec{m} = -\vec{M}/2, ..., \vec{M}/2 - \vec{1}$.

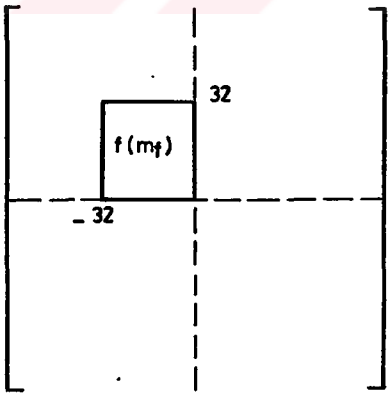

Figure 4.1: Schematic representation of $g(\vec{m})$.

In order to avoid an overlap of the signal and its twin, one must choose $m_0 > M_f/2$ or $n_0 > N_f/2$ or both [19]. By means of the Fast Fourier Transform (FFT),

the discrete spectrum $G(\vec{k}) = DFT[g(\vec{m})]$ is computed. The imaginary part of $G(\vec{k})$ is discarded. A constant bias B is added to the real part of $G(\vec{k})$ to get the discrete hologram distribution

$$H(\vec{k}) = Re[G(\vec{k})] + B = \mid F(\vec{k}) \mid \cos[2\pi \vec{k} \cdot \vec{m}/\vec{M}] + B \tag{4.4}$$

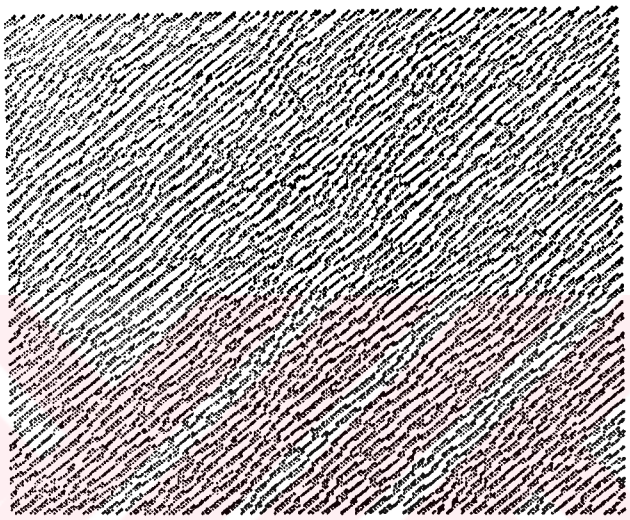

Figure 4.2: Hologram distribution of the signal " F ".

The distribution $H(\vec{k})$ is real and positive valued and is suitable to produce the digital hologram. Fig[4.2] shows a typical example of Fourier transform hologram of the signal " F ".

This hologram is produced under the following conditions that if $H(\vec{k})$ is greater than zero " / " character is printed, while a blank space is left if it is less than zero.

Fig[4.3] shows topological graph of the $Re[G(\vec{k})]$ of the signal " F ".

The distribution, Fig[4.2], was printed on a paper then photoreduced on high resolution hologram plates to dimensions $1x1cm$. The optical reconstruction is realized by the optical set-up shown in Fig[4.4]. The CGH is illuminated by a He-Ne laser and then Fourier transformed by a lens at its back focal plane where the desired

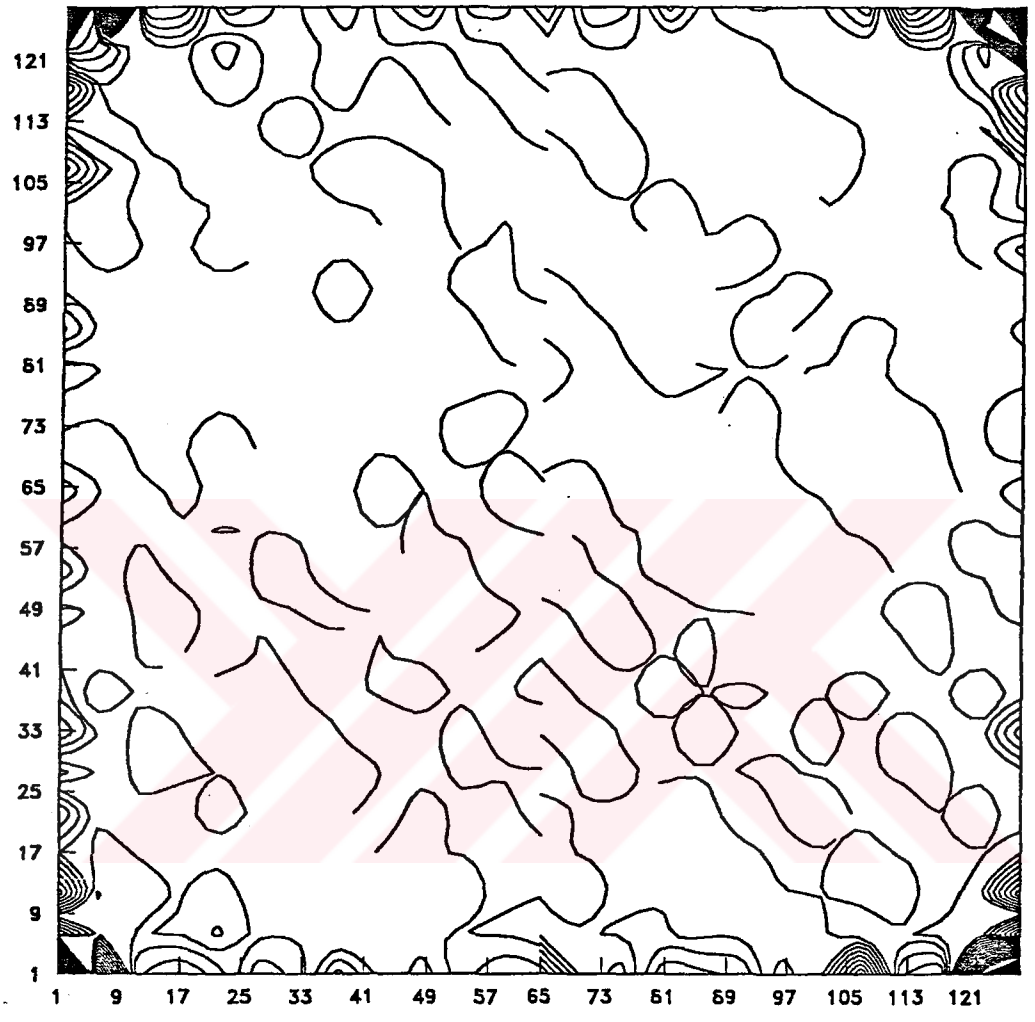

Figure 4.3: Topological graph of the $Re[G(\vec{k})]$ values of the signal " F ".

image is reconstructed.

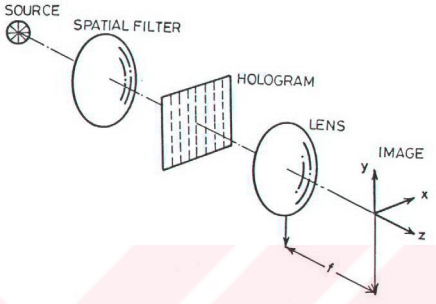

Figure 4.4: Optical reconstruction set-up.

Figure 4.5: Reconstructed image of the signal " F ".

Since the amplitude of the computer generated light disturbance for the Fourier transform of a signal is quantized by applying a threshold value, the dc (or zero order) and low spatial frequency components of the signal, which are much larger than those of the high spatial frequency components, are lost considerably. This effect is

obvious in the topological graph. Topological graphs are drawn by Surfer which is a 3-dimensional pocket graph program. Since the program is not able to process such a large matrix, it is divided into two parts in the form of ((0,1,...,64),(0,1,...,127),$G(\vec{k})$) and ((65,66,...,127),(0,1,...,127),$G(\vec{k})$). Then resulting two graphs are joint together. Due to this operation some of the contours at the limit remained open. However, this has of not much importance, because all the portions of the hologram carries complete information about the object. The values of the matrices are relabelled by the program with 0.2 intervals and then contours are drawn between the neighboring points. The high pass filtering effect appears in the optically reconstructed image.

4.3 Application of Phase Freedom : Diffuser

In order to reduce this high pass filtering effect, which is observed in the previous case or to smooth the spectrum we defined $f(\vec{m})$ in Eq[4.3] as

$$f(\vec{m}) = \mid f(\vec{m}) \mid e^{i\phi} \tag{4.5}$$

where phase angle ϕ is a free parameter generated by the computer as random numbers between the limits

$$-\pi < \phi < \pi \tag{4.6}$$

This procedure of adding the random phase factor to the signal is quite identical to placing a diffuser in front of the object in optical holography. However, the multiplication of the random factor to the signal causes deterioration of the optically reconstructed image due to the random noise of the diffuser.

In this case Eq[4.4] takes the form

$$H(\vec{k}) = Re[G(\vec{k})] + B = \mid F(\vec{k}) \mid \cos[2\pi\vec{k}\cdot\vec{m}/\vec{M} + \phi(\vec{k})] + B \tag{4.7}$$

and hardcliping operator was applied. For $H(\vec{k}) < 0$ we left a space and for $H(\vec{k}) > 0$ " / " was printed.

Fig[4.6] and Fig[4.7] show the hologram distribution and the reconstructed image, Fig[4.8] shows the topological graph of $Re[G(\vec{k})]$ values.

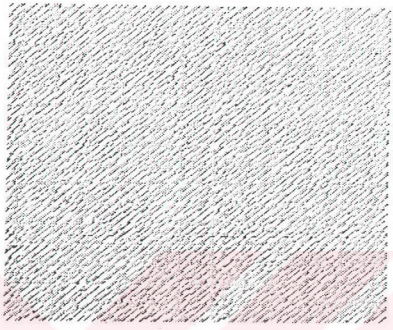

Figure 4.6: Hologram distribution of phase added signal " F ".

Figure 4.7: Reconstructed image of the random phase added signal " F ".

From these holograms it is recognized that the spectrum of the hologram is smoother than the phaseless case and high pass filtering effect which is observed in the image of Fig[4.3] disappeared, but its quality deteriorated due to the random noise. Consequently a large amount of Fourier transform components of the signal is extremely uniformly distributed over the whole hologram.

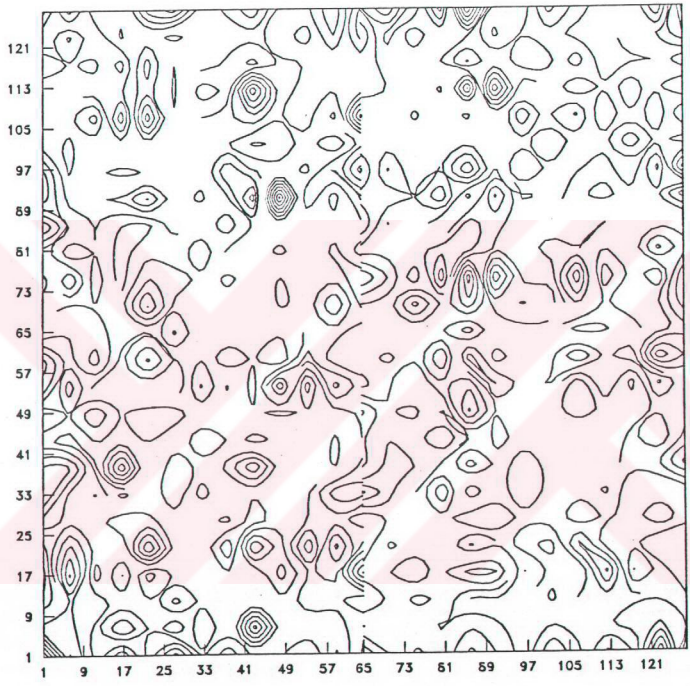

Figure 4.8: Topological graph of $Re[G(\vec{k})]$ values of phase added signal " F ".

In conclusion to code the complex amplitude $F(\vec{u})$ successfully , it is necessary

i) to find and formulate the existing freedoms,

ii) to develop a coding scheme which is able to use these freedoms to convert $F(\vec{u})$ to $G(\vec{u})$ without or with only minor deterioration of the original object information.

4.4 Application of Diagonal Method

To show the effect of the hologram structure on the reconstructed image letter " E " was sampled and its distribution was calculated according to Eq[4.6]. First hardcliping operator was applied as for $H(\vec{k}) < 0$ we left a space and for $H(\vec{k}) > 0$ "." printed. The distribution and reconstructed image is shown in Fig[4.9].

In Fig[4.9] hologram gives a noisy cloud around the zero order term, several diffracted orders are obtained. In the resulting hologram distribution existence of diagonal fringes are observed, then the diagonal points are connected. The resulting hologram and the reconstructed images are shown in Fig[4.10].

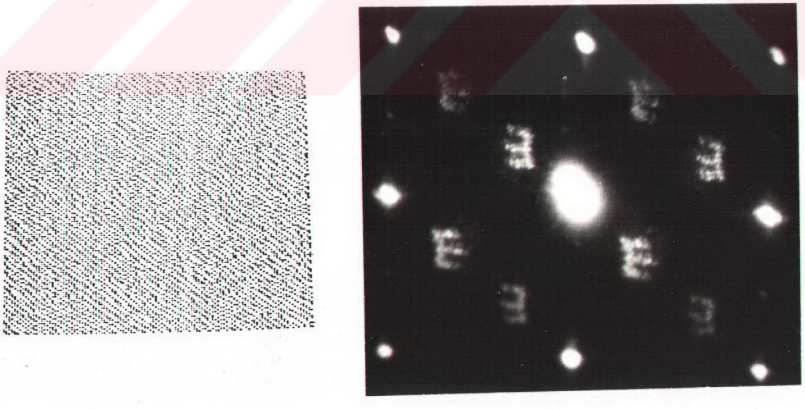

Figure 4.9: Hologram distribution and the reconstructed image of the signal " E ".

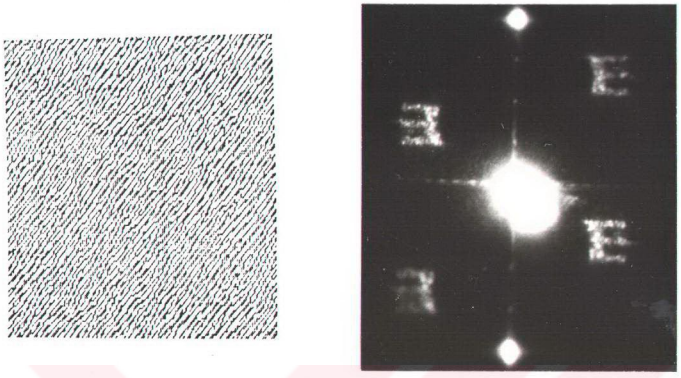

Figure 4.10: Hologram distribution and the reconstructed image of the signal " E " after applying the diagonal method.

Diagonal method causes a clear orientation of the weak higher order images as shown in Fig[4.10].

Chapter 5

Iterative Fourier Transform Algorithm Applied To Digital Amplitude Holograms

5.1 Introduction

The process for producing computer generated holograms (CGH's) is flexible and permits manipulation of several parameters. In numerous applications only the reconstructed intensity distribution is of concern. Then, a powerful and interesting possibility is to superpose a suitable phase distribution onto the input data. In contrast to optical holography, any desired phase distribution is possible in computer generated holography.

Superposing a phase onto the data represented by an amplitude distribution will influence the spectrum of this distribution. Because of the synthetic production of CGH's the incorporation of an artificial diffuser is easy to accomplish. The freedom to choose an appropriate phase distribution to superpose the input data may be used as follows :

1) to smooth the amplitude distribution across the spectrum,

2) to improve the resistance of data against imperfections such as dirt and scratches in the CGH.

The diffraction efficiency of Fourier holograms is increased by smoothing the spectrum [20,21,22]. The insensitivity against defects is of particular interest in a

holographic storage systems. In general, a random phase distribution is introduced to achieve these goals.

The superposition of a random phase in computer holography is equivalent to the introduction of a diffuser, e.g., a ground glass in optical holography. An optical Fourier hologram produced in this way possesses the property that the data are reconstructed although part of the hologram is bleached. However, a decrease of brightness as well as resolution will occur. Unfortunately, the incorporation of a random phase introduces speckles into the reconstruction.

The aim in digital amplitude holography is to calculate and to fabricate a transparency, a digital hologram, that is able to cause a diffraction pattern of which a specified light distribution is a part. The problem in finding this hologram does not have a unique solution. Several hologram distributions can reconstruct the desired signal. However, they have different diffraction efficiencies. To characterize these holograms we start from a specific hologram distribution and interpret all the other holograms of the same signal as modifications of this basic one.

Iterative Fourier Transform Algorithms (IFTA) are used to solve the problems in a number of fields, e.g., astronomy, wavefront sensing, electron microscopy, and crystallography [23,24].

When analytical methods fail, it is often possible to solve the problem by an iterative method. A synthesis problem typically arises when one wants the Fourier transform of an object (or a signal,aperture, antenna array, etc.) to have certain desirable properties. There may not exist a Fourier transform that is completely desirable and satisfies all the constraints. Nevertheless, one seeks a Fourier transform pair that comes as close as possible to having the desirable properties and satisfying the constraints in both domains.

The information available in any one domain is insufficient to reconstruct the object or its complex Fourier transform. The problem can be expressed as follows

[25]: given a set of constraints placed on an object and another set of constraints placed on its Fourier transform, find a Fourier transform pair (i.e.,an object and its Fourier transform) that satisfies both sets of constraints.

Once a solution is found to a such problem, the question remains: is the solution unique? For synthesis problems, the uniqueness is usually unimportant. One is satisfied with any solution that satisfies all the constraints; often a more important problem is whether there exists any solution that satisfies what may be arbitrary and conflicting constraints.

5.2 Application of IFTA to Digital Amplitude Holograms

The iterative method that we describe show results of the experiments applying the problem of reduction of quantization noise in computer generated holograms.

The analog hologram distribution $G(\vec{u})$ is given as

$$G(\vec{u}) = \mid F(\vec{u}) \mid \cos[2\pi\vec{u}\cdot\vec{x} - \Phi(\vec{u})] + B \tag{5.1}$$

where $B = -F_{min} = -min\{F(\vec{u})\cos[2\pi\vec{u}\cdot\vec{x} - \Phi(\vec{u})]\}$. This distribution results in reconstruction

$$f(\vec{x}) = \frac{1}{2}f(\vec{x} - \vec{x_0}) + \frac{1}{2}f^*[-(\vec{x} + \vec{x_0})] + B\delta(\vec{x}) \tag{5.2}$$

The quantization of $G(\vec{u})$ into two discrete levels can be expressed as with the quantization operator

$$QZ[G(\vec{u})] = \begin{cases} 0 & G(\vec{u}) \leq 1/2 \\ 1 & 1/2 < G(\vec{u}) \end{cases}$$

and

$$QZ[G(\vec{u})] = \bar{G}(\vec{u}) \tag{5.3}$$

To examine the effect of QZ on the reconstructed signal the term

$$Q(\vec{u}) = \bar{G}(\vec{u}) - G(\vec{u}) \tag{5.4}$$

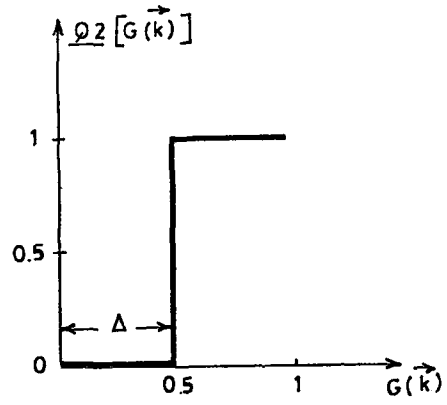

Figure 5.1: Illustration of the quantization operator

is introduced. $Q(\vec{u})$ describes the change in the hologram plane which is caused by QZ. The reconstruction of the quantized hologram is then

$$f(\vec{x}) = g(\vec{x}) + q(\vec{x}) = \frac{1}{2}f(\vec{x} - \vec{x_0}) + \frac{1}{2}f^*[-(\vec{x} + \vec{x_0})] + B\delta(\vec{x}) + q(\vec{x}) \qquad (5.5)$$

Figs[4.9] and [4.10] show a hologram distribution which was binarized with $Q2$ and its reconstruction $\bar{g}(\vec{x})$ respectively. Signal disturbances are caused by the parts of the quantization noise $q(\vec{x})$ in the signal window. To obtain an undisturbed signal it is necessary to ensure $q(x) = 0$ in the signal window. When the intensity $i(\vec{x}) = \mid f(\vec{x}) \mid^2$ is the desired signal another strategy to avoid quantization errors exists. The quantization noise $q(\vec{x})$ can be adjusted to the complex amplitude $f(\vec{x} - \vec{x_0})$ in such a way that

$$\mid f(\vec{x} - \vec{x_0}) + q(\vec{x}) \mid^2 \sim i(\vec{x} - \vec{x_0}) \qquad (5.6)$$

It is not necessary to require $q(\vec{x}) = 0$ in the signal window to fulfill Eq[5.6] because the phase of $[f(\vec{x} - \vec{x_0}) + q(\vec{x})]$ can be chosen freely.

Starting from the distribution $G(\vec{u})$ and the reconstruction $g(\vec{x})$, a Fourier pair $\bar{g}(\vec{x}) \leftarrow FT \rightarrow \bar{G}(\vec{u})$ is to synthesize, which possesses the properties

i) $\bar{G}(\vec{u})$ is quantized into Z levels and

ii) $\bar{g}(\vec{x})$ contain the signal $i(\vec{x})$, i.e.,$\mid g(\vec{x}) \mid^2 \sim i(\vec{x})$ in the signal window.

To implement the synthesis of the Fourier pair $\bar{g}(\vec{x}) \leftarrow FT \rightarrow \bar{G}(\vec{u})$ the initial distribution

$$g_0(\vec{x}) = \mid f(\vec{x}) \mid e^{i\phi(\vec{x})} \tag{5.7}$$

with the random phase $\phi(\vec{x})$ is introduced. The operator X was to ensure the constraints in the signal plane and the operator U the constraints in the hologram plane.

The operators U and X mathematically describe the rules to fulfill the constraints in the $\vec{x}$ and $\vec{u}$ planes. With a suitable choice of the operators a convergent iteration can be expected. Convergence of an IFTA means that, after J iteration cycles, a distribution $\bar{g}_J(\vec{x})$ is found which fulfills the constraints in the $\vec{x}$ plane better than the distribution $\bar{g}_1(\vec{x})$, i.e., the algorithm reduces the error.

The operator X is

$$X[\bar{g}_j(\vec{x})] = \begin{cases} g_j(\vec{x}) & x \in f(\vec{x}) \\ 0 & \text{otherwise} \end{cases}$$

and $X[\bar{g}_j(\vec{x})] = g_{j+1}$.

If the other operator U is used as stated in Eq[5.3] the iteration stagnates after a few iteration. In order to overcome the stagnation the quantization operator is introduced stepwise.

$$U2^p[G_j(\vec{k})] = \begin{cases} 0 & \text{if } G_j(\vec{k}) \leq \epsilon^{(p)} \\ 1 & \text{if } 1 - \epsilon^p < G_j(\vec{k}) \\ G(\vec{k}) & \text{otherwise} \end{cases}$$

and $U2^p[G_j(\vec{k})] = \bar{G}_j(\vec{k})$.

The values of the parameters are ;

$p = 1, 2, ..., 10$, $j = 5$, and, $\epsilon^{(1)} = 0.15$, $\epsilon^{(2)} = 0.25$ $\epsilon^{(3)} = 0.30$, $\epsilon^{(4)} = 0.35$, $\epsilon^{(5)} = 0.375$, $\epsilon^{(6)} = 0.40$, $\epsilon^{(7)} = 0.425$, $\epsilon^{(8)} = 0.450$, $\epsilon^{(9)} = 0.475$, and the last step run only one

cycle.

$$U2^{(10)}[G_9(\vec{k})] = \begin{cases} 0 & \text{if } G_{10}(\vec{k}) \leq 0.5 \\ 1 & \text{if } 0.5 < G_{10}(\vec{k}) \end{cases}$$

and $U2^{(10)}[G_9(\vec{k})] = \bar{G}_{10}(\vec{k})$.

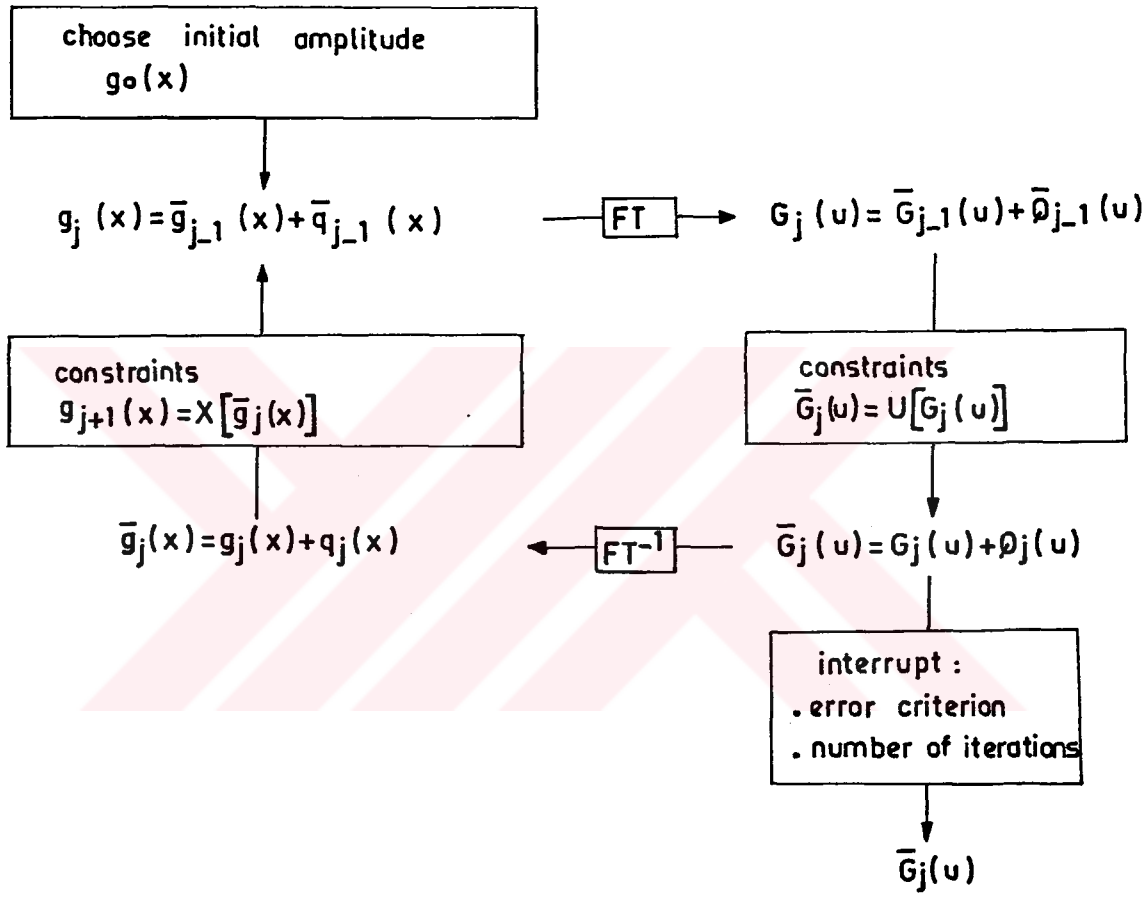

Figure 5.2: Illustration of the iterative Fourier transform algorithm.

The algorithm is shown in Fig[5.2] and for implementation of the program see Appendix A.

The graph of $U2^p$ operator is shown in Fig[5.3].

The optimal value of p was found empirically. A recent work reported by

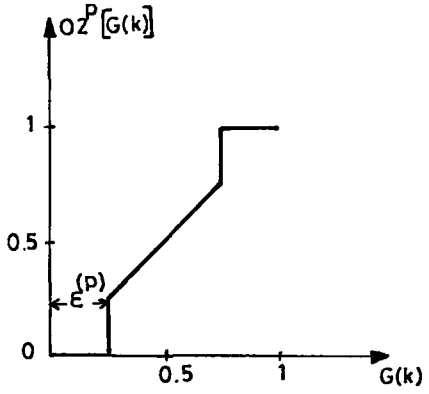

Figure 5.3: Graph of $U2^p$.

Wyrowski [27] showed that a similar algorithm can be used to produce CGH's of good quality and high diffraction efficiency.

In Wyrowski's work the object and its twin are implemented in the data matrix together. But M/M_f ratio should be equal to or greater than 8 to separate the signal and its twin in the reconstruction plane. This requirement was met by using large data matrix.

In the case of continuous intensity objects the phase freedom is severely limited and iterative quantization methods seem not to be appropriate.

Due to a stepwise introduction of the constraints in the Fourier plane a stagnation is avoided. The experimental results demonstrate that it is possible to produce quantized holograms which generate signal reconstructions with small quantization errors.

Fig[5.3] shows the hologram distribution, Fig[5.4] the reconstructed image and Fig[5.5] is the topological graph of $Re[G(\vec{k})]$.

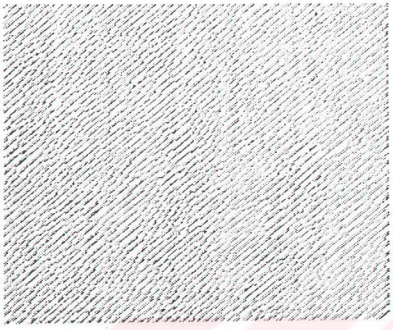

Figure 5.4: Hologram distribution of the signal " F " after iteration.

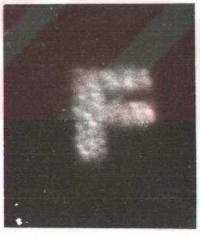

Figure 5.5: Reconstructed image of the signal after applying IFTA.

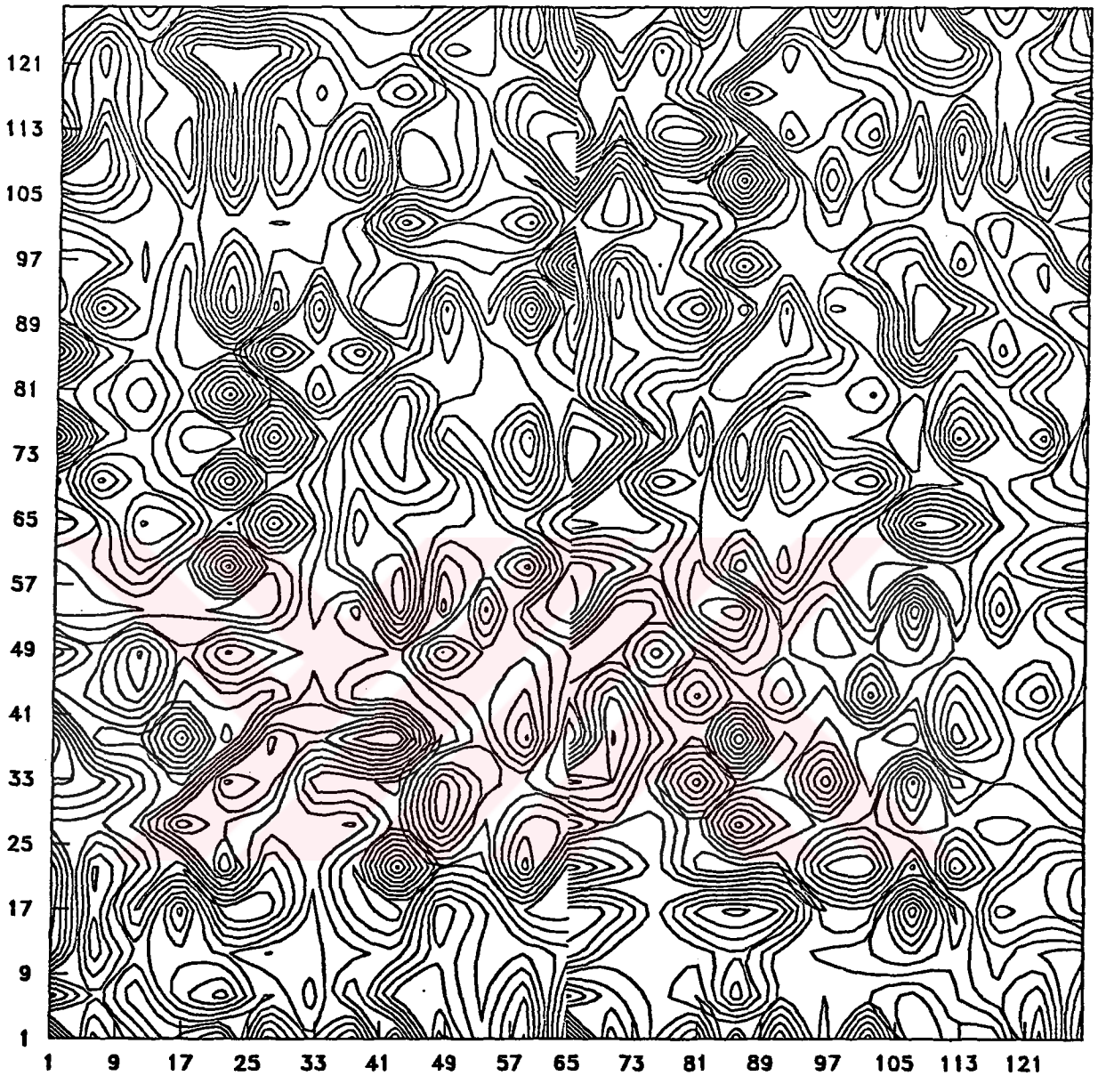

Figure 5.6: Topological graph of $Re[\bar{G}(\vec{k})]$ values of the signal after iteration.

Chapter 6

Recording of the CGH Distributions on Al

For the mass production of optical elements the calculated CGH patterns are mostly recorded on Al or Cr through photoresist instead of photographic plates. In this chapter procedure of recording of the hologram distributions on Al is explained [28,29,30].

The schematic flowchart of the process is shown in Fig[6.1].

6.1 Substrate Preparation

Microscopic slides were used as substrate. They are cleared chemically as follows :

-Boil in detergent for 5 *min*

-Wait in HCl 5 *min* then wash in DI water by means of ultrasonic agitator for 2 *min*

-Wash with aceton for 15 *min* then dry by blow drying with filtered nitrogen.

After drying process the substrate is put into vacuum evaporator, then Al is evaporated in the vacuum system under 10^{-6} *torr* pressure.

6.2 Photolithography

- Photoresist coating :

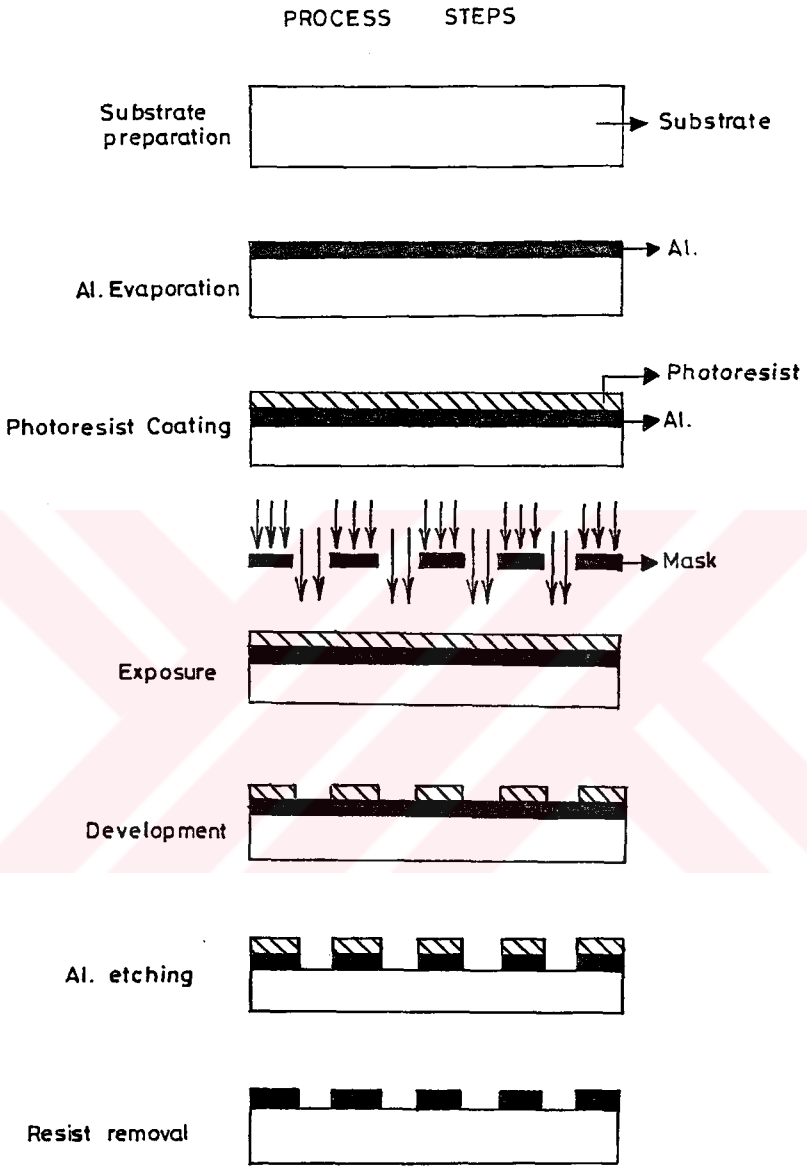

Figure 6.1: Flowchart of the process.

AZ1350 of Shipley Co. is used as a photoresist which is sensitive to UV radiation and gives positive images. Photoresist is coated on Al by spin coated method with 4200 *rpm* spin speed for 30 *sec.* The relation between the thickness and spin is shown in Fig[6.2].

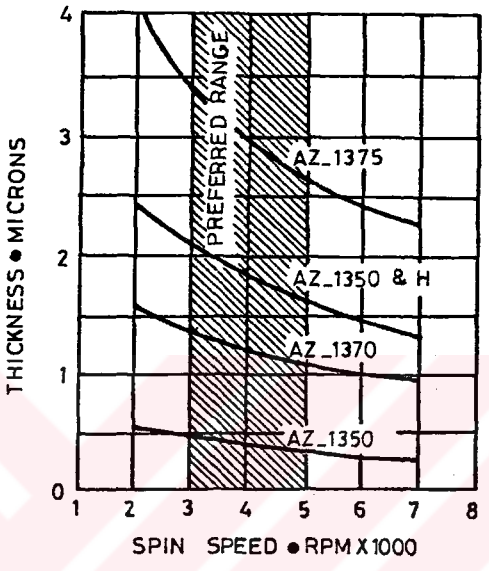

Figure 6.2: Photoresist thickness on Al versus spin speed graph.

- Softbake :

Softbaking is the process step where in almost all the solvents are removed from the photoresist coating, rendering it photosensitive. The samples are heated at $70°C$ for 25 *min* under nitrogen ambient to make them sensitive to UV before exposure.

- Exposure :

In this step the samples were exposed to UV through previously calculated CGH distribution for 8 *s* using mask aligner.

- Development :

The photoresist is developed for 30 *s* in developer solution which has 1 part H_2O and 1 part MF312 developer of Shipley Co. Then washed in DI water for 2 *min* and spin dried.

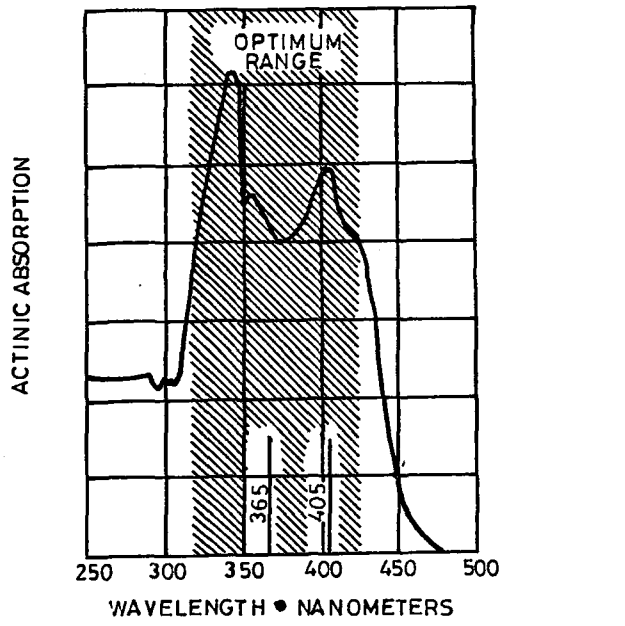

Figure 6.3: Atomic absorption versus wavelength graph.

- Postbaking :

It is rebaked at $95°C$ under nitrogen for 10 *min* to resist to etching solution.

- Al etching :

Al etching is achieved in orthophosphoric acid (H_3PO_4) for 8 *min*, then washed in DI water and dried.

- Photoresist removal :

The photoresist on CGH pattern is removed by immersing the hologram in acetone.

The CGH is then put into the reconstruction set-up and the result is shown in Fig[6.4]. The optical resolution is found about 1 μm.

The speckles are due to the poor Al coating and Al etching. For better coating electron beam evaporation systems of Al can be used. Poor Al coverage causes voids and cracks that are too small to be protected by the next photoresist coating step. When the aluminum etched these areas are attacked, creating greater voids. Also

plasma aluminum etching is superior to wet etching because it provides a less aggressive chemistry to the photoresist image and generally offers reduce under cutting compared with wet acid etchents.

To produce high quality optical elements the resolution requirements are met, but it is necessary to use new techniques for coating and etching steps.

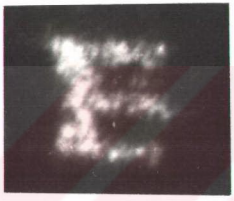

Figure 6.4: Reconstructed image of the hologram distribution recorded on Al.

Chapter 7

Conclusion

In general, amplitude holograms possess lower diffraction efficiency than phase holograms. However, amplitude holograms are interesting in several aspects :

1) their easy production,

2) their quality of reconstruction independently of wavelength,

3) their utility as a starting point in constructing highly efficient volume holograms.

The aim in digital amplitude hologram is to calculate and produce a transparency - the digital hologram, that is able to cause a diffraction pattern of which a specified light distribution, i.e., signal is a part.

In this work, we simulated the optical off axis hologram. The object is sampled in a 32x32 matrix. Then the object matrix is placed in a data matrix of 128x128 dimensions for numerical calculation of its Fourier spectrum. The placement and dimensions of the object matrix should satisfy some restrictions, i.e., $m_0 > M_f/2$ and/or $n_0 > N_f/2$ to avoid an overlap of the signal and its twin.

The Fraunhofer diffraction pattern of the object is given as a Fourier transform of the data matrix. FT of the matrix was calculated by FFT algorithm. The one dimensional FFT algorithm based on successive doubling method was adapted to two dimensionals. It is not the most efficient algorithm but is convenient for our purposes and programs.

In general, the spectrum $G(\vec{k})$ is a complex valued distribution. Therefore, it is necessary to encode $G(\vec{k})$ in a real and positive valued distribution. The use of constant bias like a reference wave as in the case of optical holography is a way to encode the Fourier spectrum. The advantage of this method the noise component in the reconstruction is just a plane wave.

The constant bias was added to the real part of $G(\vec{k})$ to get hologram distribution, then hardclip operator was applied to quantize the amplitude of the computer generated light disturbance for the Fourier transform of a signal.

The quantized distribution was printed on a paper, and photoreduced on a high resolution photographic plates to produce computer generated hologram.

The reconstruction is realized by a special optical set-up.

The high pass filtering effect appears in the optically reconstructed images. To eliminate this high pass filtering effect, i.e., to smooth the spectrum or dynamic range, the elements of data matrix were multiplied by random phase factors. This procedure is identical to placing a diffuser in front of the object in optical holography. But the holograms obtained in this way, due to the random noise of the diffuser, has deteriorated optically reconstructed images.

To raise hologram quality and reduce quantization errors, instead of hardclip operator, an iterative method, which introduces the operator stepwise, is developed and applied to the signal with restrictions on both domain. To do this well known IFTA techniques are employed. The problem in this case is to find a hologram which does not have a unique solution. Several hologram distributions can reconstruct the desired signal but they have different qualities. So we started from a specific hologram distribution and interpreted all the other holograms of the same signal as a modification of this basic one. The parameters, i.e. number of cycles and form of the operator etc., should be determined by taking into consideration the signal. From the stepwise introduction of the quantization constraint follows an increased capability

of the IFTA to change the hologram distribution during the iteration in such away that the quantization errors in the reconstruction plane are reduced.

In the hologram structure, the existence of the diagonal fringes are observed and when this diagonal points are connected the higher diffraction order images are eliminated in the reconstruction.

The CGH's are being used as optical elements, e.g. in CD's drivers, so their production on Cr or Al is important. In the last chapter, a photolithographic method is explained in detail to record hologram distribution on Al.

In general, CGHs function as a diffractive elements in optical systems, therefore the hologram to be used by a machine has very different requirements. The wavefront produced by such a hologram need not be bright, or cosmetically attractive. On the other hand, it must be accurate. As a result, besides the software development for coding the hologram structure, hardware requirements should be met to produce higher quality computer generated holograms.

The resolution required varies from $0.2\mu\ m$ to $10\mu\ m$ depending on the application. With increasing demand of structure detail in the order of wavelength used in the reconstruction, drum and flat bed laser scanners are used to create exposure patterns onto photosensitive materials in the right scale.

As the dimensions required are comparable with IC patterns the same or similar systems may be used in the production of CGHs. Electron beam lithography systems and ion exchange techniques are already being used in this field.

LIST OF REFERENCES

[1] Brown, B. R., and A. W. Lohmann, 1966, Appl. Opt. **5**, 967.

[2] Bryngdahl O., and F. Wyrowski, 1990, in Progress In Optics Vol. XXVIII, ed. E. Wolf (North - Holland, Amsterdam) pp. 1-86.

[3] Burch, J. J., 1967, Proc. IEEE **55**, 599.

[4] Akahori, H., 1973, Appl. Opt. **12**, 2336.

[5] Lesem, L. B., P. M. Hirch and J. A. Jordan Jr, 1967, Proc. Symp. Modern Optics, Vol. 17 (Polytechnic Institude of Brooklyn, New - York) pp. 681.

[6] Lee, W. H., 1970, Appl. Opt. **9**, 639.

[7] Lee, W. H., 1978, in Progress In Optics, Vol. XVI, ed. E. Wolf (North - Holland, Amsterdam) pp. 119-232.

[8] Wyrowski, F., 1989, Appl. Opt. **28**, 3864.

[9] Huang, T. S., 1971, Proc. IEEE **59**, 1335.

[10] Yaroslovskii, L. P., and N. S. Merzlyakov, 1980, Methods Of Digital Holography (Plenum Press, New - York).

[11] Dallas, W. J., 1980, in The Computer In Optical Research, Topics in Applied Physics, Vol. 41, ed. B. R. Friedem (Springer, Berlin) pp. 291-366.

[12] Schreier, P., 1984, Synthetische Holograpie (VEB, Leibzig).

[13] Tricolas, G., 1987, Appl. Opt. **26**, 4351.

[14] Hecht, E., and A. Zajac, 1977, Optics (Addison - Wesley, New - York) pp. 347.

[15] Goodman, W. J., 1968, Introduction To Fourier Optics, (Mc - Graw Hill, New - York), pp. 50.

[16] Whittaker, E. T., 1915, Proc. Roy. Soc. Edinburg, Sec.**A35**, 181.

[17] Shannon, L. E., 1949, Proc. IRE **37**, 10.

[18] Cooley, J. W, P. A. W. Lewis, and P. D. Welch, 1969, IEEE Trans. Educ. **E-12**, no. 1, 27.

[19] Wyrowski, F., and O. Bryngdahl, 1989, J. Opt. Soc. Am. **A6**, 1171.

[20] Akahori, H., 1986, Appl. Opt. **25**, 802.

[21] Wyrowski, F., R. Hauck and O. Bryngdahl, 1987, J. Opt. Soc. Am. **A4**, 694.

[22] Wyrowski, F., and, O. Bryngdahl, 1988, J. Opt. Soc. Am. **A5**, 1058.

[23] Gerchberg, R. W., and W. O. Saxton, 1972, Optik **35**, 237.

[24] Fienup, J. R., 1982, Appl. Opt. **21**, 2758.

[25] Fienup, J. R., 1980, Opt. Eng, **29**, 297.

[26] Wyrowski, F., 1989, Appl. Opt. **28**, 3864.

[27] Wyrowski, F., 1990, J. Opt. Soc. Am. **A7**, 383.

[28] Loops, P., 1990, Philips J. Res. **44**, 481.

[29] Elliot, D. J., 1982, Integrated Circuit Fabrication Technology, (Mc - Graw Hill, New - York).

[30] Technical Data Sheet of AZ-1300 Series, Shipley Co.

Appendix A

Flowchart of IFTA

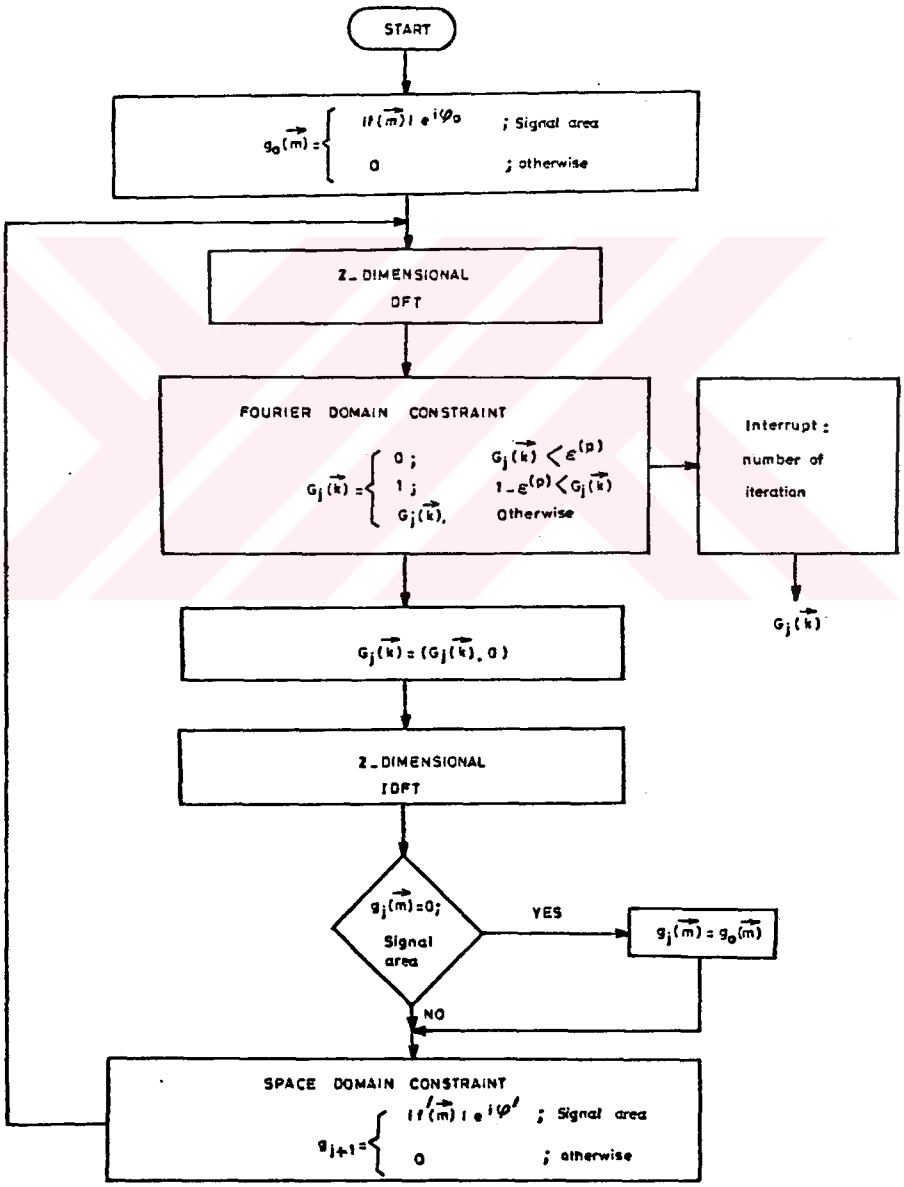

VITA

Nationality : Turkish citizen.

Educational background : B.Sc. in Physics, METU, Ankara, 1983.

M.Sc. in Physics, METU,Ankara, 1986.

Ph.D. in Physics, METU, Ankara, 1991.

Employment : Research assistant, Department of Physics, METU,

1984-present.